Journal of Thermal Analysis and Calorimetry (2022) 147:7917–7944
https://doi.org/10.1007/s10973-021-11080-y

Thermal entropy generation and exergy efficiency analyses of coiled wire inserted nanodiamond + Fe_3O_4/water hybrid nanofluid in a tube

L. Syam Sundar[1] · Solomon Mesfin[2] · E. Venkata Raman[3] · V. Punnaiah[4] · Ali J. Chamkha[5] · António C. M. Sousa[1]

Received: 14 July 2021 / Accepted: 15 September 2021 / Published online: 9 October 2021

Abstract

Exergy efficiency, Nusselt number, friction factor, pressure drop, thermal and frictional entropy generation of water-based nanodiamond + Fe_3O_4 nanofluid flow in a tube and with various coiled wire inserts have been studied experimentally under turbulent and constant heat flux boundary conditions. The experiments were conducted in the Reynolds number range from 2000 to 22,000, particle concentrations of 0.05%, 0.1% and 0.2% and coiled wire inserts of different p/d values of 3.67, 2.34 and 1.00, respectively. Results indicate that at 0.2% vol. and Reynolds number of 20,095, without coiled wire inserts, the heat transfer coefficient, Nusselt number, friction factor, pressure drop and pumping power are enhanced to 44.36%, 29.55%, 11.1%, 29.58% and 39.49% over the base fluid data. Similarly, at 0.2% vol. and Reynolds number of 20,095, with coiled wire inserts of $p/d = 1$, the heat transfer coefficient, Nusselt number, friction factor, pressure drop and pumping power are further enhanced to 107.19%, 66.36%, 38.84, 64.44% and 76.54% over the base fluid data without inserts. The thermal entropy generation is decreased to 30.80% and it is further decreased to 46.34% at 0.2% vol. and Reynolds number of 20,095 with coiled wire inserts of $p/d = 1$. The exergy efficiency of water is 18.95%, and it is increased to 24.06% for 0.2% vol. and it is further increased to 51.85% for 0.2% vol. and Reynolds number of 20,095 with coiled wire inserts of $p/d = 1$. The study indicates that the hybrid nanofluids with coiled wire inserts are guaranteed choice for augmenting the exergy efficiency of flow through tube.

Keywords Hybrid nanoparticles · Heat transfer · Nusselt number · Exergy · Entropy generation

Abbreviations

A	Area, m^2
Be	Bejan number
D	Inner diameter, m
D_o	Outer diameter, m
d_h	Hydraulic diameter, m
f	Friction factor
g	Acceleration due to gravity, m s^{-2}
H	Manometric fluid height, m
h	Heat transfer coefficient, W m^{-2} k^{-1}
k	Thermal conductivity, W m^{-2} k^{-1}
L	Length of the tube, m
$\dot{m}$	Mass flow rate, kg s^{-1}
Ns	Entropy generation number
Nu	Nusselt number, hD/k
p	Pitch of the coiled wire, m
Pp	Pumping power, W
Pr	Prandtl number, $\mu \times C_p/k$
Q_h	Rate of heat supplied to the test tube, W
Q_a	Rate of heat absorbed by the fluid, W
Q_{avg}	Average rate of heat, W
Re	Reynolds number, $4\dot{m}/\pi D_i \mu$
$\dot{S}_{g,H}$	Thermal entropy generation, W k^{-1}
$\dot{S}_{g,F}$	Frictional entropy generation, W k^{-1}
t	Thickness of the coiled wire, m
T	Temperature, °C
v	Velocity of the fluid, m s^{-1}

✉ L. Syam Sundar
sslingala@gmail.com

1 Centre for Mechanical Technology and Automation (TEMA-UA), Department of Mechanical Engineering, University of Aveiro, 3810-193 Aveiro, Portugal

2 Department of Mechanical Engineering, University of Gondar, Gondar, Ethiopia

3 I3N, Department of Physics, University of Aveiro, 3810-193 Aveiro, Portugal

4 Electrical Engineering Section, Engineering Department, Center for DNA Fingerprinting and Diagnostics (CDFD), Department of Biotechnology, MoS&T, Hyderabad, India

5 Faculty of Engineering, Kuwait College of Science and Technology, 35004 Doha District, Kuwait

Subscripts

i	Inlet
o	Outlet
m	Mean
s	Surface

Symbols

ρ	Density, kg m^{-3}
ϕ	Particle volume concentration, %
ΔP	Pressure drop, Pa
μ	Viscosity, mPa.s
η	Thermal performance factor

Introduction

The invented nanofluid of Choi [1] gives the enhanced thermal conductivity, which causes the enhanced heat transfer coefficients, while they flow in thermal equipments. Nanofluids have superior thermal conductivity than the single-phase fluids. Esfe et al. [2] have obtained the enhanced thermal conductivity of water–titania nanofluids with an increase in temperature and particle volume concentration based on the artificial neural network. Riahi et al. [3] prepared Al_2O_3–water nanofluids using pulsed laser ablation technique in liquid and analyzed the thermal conductivity of nanofluids. They have observed increase in thermal conductivity of nanofluids with an increase in temperature and particle volume loadings. Li et al. [4] developed an empirical correlation for the thermal conductivity of SiO_2-oleic acid/liquid paraffin nanofluid with a deviation less than 10%. Sundar et al. [5] have obtained the thermal conductivity and viscosity enhancements of 48% and 2.96 times of 2.0% volume concentration of Fe_3O_4/water nanofluid at 60 °C compared to base fluid. Liu et al. [6] noticed thermal conductivity enhancement of 22.4% at 0.05% vol. of CuO/water nanofluid. Guo et al. [7] found thermal conductivity increases of 3.2% and 9.6% for 0.5 vol.% of SiO_2-EG and 1.0 vol. % of SiO_2-EG than the base fluid. Due to the nanoparticle migration, Brownian motion and micro-convection, the nanofluids offer higher thermal conductivity values.

Researchers have noticed heat transfer coefficient enhancements for nanofluids flow in a forced convection apparatus. Sundar et al. [8] revealed Nusselt number and friction factor increase of 39.18% and 19.12% at 0.6% vol. of Ni/water nanofluid flow in a forced convection apparatus under turbulent flow compared to water. Ali [9] found an increase in heat transfer coefficient by 27% at 0.007% vol. of SiO_2/water nanofluid flow in a forced convection apparatus under turbulent flow. Kim et al. [10] noticed heat transfer coefficient enhancement of 160% for flow of Al_2O_3/water nanofluid in a 0.8-mm-diameter tube compared to 2.0-mm-diameter tube at a Reynolds number of 1588.

Azeez et al. [11] numerically evaluated that heat transfer coefficient and pressure drop of Al_2O_3/water nanofluid flow in a double-pipe heat exchanger in the Reynolds number range from 5000 to 30,000 in the particle loadings from 1 to 4% using ANSYS software and observed higher heat transfer coefficients. Azmi et al. [12] conducted heat transfer experiments for water-based TiO_2 and SiO_2 nanofluids flow in a tube and obtained heat transfer coefficient increase of 26% at 1.0% vol. of TiO_2 nanofluid and heat transfer coefficient increase of 33% at 3.0% vol. of SiO_2 nanofluid. Duangthongsuk and Wongwises [13] observed heat transfer coefficient enhancement of 6–11% for TiO_2–water nanofluid flow in a double-pipe heat exchanger under turbulent flow. Albadr et al. [14] conducted heat transfer experiments for Al_2O_3–water nanofluid flow in a shell and tube heat exchanger under turbulent flow and observed an increase in heat transfer coefficients compared to water. Godson et al. [15] noticed heat transfer coefficient increase of 12.4% and effectiveness of 6.14% for 0.04% vol. of silver/water nanofluid flow in a shell and tube heat exchanger.

The nanofluids may be dispersion of Al_2O_3, CuO, Cu, carbon nanotubes (CNT), Fe_3O_4, SiO_2, TiO_2 and ZnO nanoparticles in the base fluids such as water (W), ethylene glycol (EG), propylene glycol (PG) and engine oil (EO). Liu et al. [16] prepared CNT/EG and CNT/synthetic engine oil nanofluids and observed thermal conductivity enhancements of 12.4% for 1.0% vol. of CNT/EG nanofluid and 30% for 2.0% vol. of CNT/synthetic engine oil nanofluid. Sundar et al. [17] prepared 50:50% mixture of ethylene glycol and water-based Al_2O_3 and CuO nanofluids and observed an increase in thermal conductivity of nanofluids with increase in particle volume concentrations and temperatures.

Under the constant tube geometry and flow rates, the heat transfer coefficient enhancement is purely dependent on the thermal conductivity of the fluid. Enhanced thermal conductivity of the fluid provides enhanced heat transfer coefficients. The hybrid thermal conductivity of nanoparticles is higher than the single nanoparticles. Hybrid nanoparticles are called as joining of two or more nanoparticles in the size of less than 100 nm. So, the dispersed hybrid nanoparticles in a fluid are called as hybrid nanofluids, which have superior thermal conductivity than the single nanoparticles-based nanofluids. Sundar et al. [18] have observed thermal conductivity enhancement of 21% and 13% for 3.03 mass% of ND-Ni/water and ND-Ni/EG hybrid nanofluids. They also observed viscosity enhancement of twofold and 1.5-fold for 3.03% of ND-Ni/water and ND-Ni/EG hybrid nanofluids. Nine et al. [19] studied thermal conductivity of Al_2O_3-MWCNTs hybrid nanofluids in the particle mass concentration from 1 to 6% and observed an increase in thermal conductivity of nanofluids. Sundar et al. [20] observed that the thermal conductivity enhancement of 0.2% volume concentration of water-based GO/Co_3O_4 hybrid nanofluid

is about 19.14% and 0.2% volume concentration of ethylene glycol-based GO/Co_3O_4 hybrid nanofluid is about 11.85% at a temperature of 60 °C. Sundar et al. [21] revealed that thermal conductivity enhancements are about 16%, 9%, 14%, 11% and 10% for water, EG, 20:80%, 40:60% and 60:40% EG/W-based ND-Co_3O_4 hybrid nanofluids at 0.15 mass% concentration and at a temperature of 60 °C.

The use of hybrid nanofluids in various heat transfer equipments may provide the higher heat transfer rates. Some of the literature is presented below. Fazeli et al. [22] have observed convective heat transfer coefficient enhancement of 85.56%, 101.25% and 139.19% of 0.1 mass% of MWCNT-CuO/water hybrid nanofluid at a volume flow rate of 14.4, 18.9 and 24.4 L min^{-1}, respectively. Zhang et al. [23] observed heat transfer performance enhancement of 35% and pressure drop increase of 12% at 3% volume concentration of Al_2O_3-CuO/water hybrid nanofluid under turbulent flow using computational fluid dynamics. Chawhan et al. [24] noticed the overall heat transfer coefficient increase from 1211.71 to 2727.38 W m^{-2} K^{-1} at 0.1% volume concentration of Ag-doped TiO_2 hybrid nanofluid flow in a minichannel heat exchanger at constant wall temperature condition at a Reynolds number of 3480. Li et al. [25] have observed that maximum convective heat transfer coefficient of SiC-MWCNTs/ethylene glycol nanofluids is 26% higher than that of pure ethylene glycol flow in a car radiator systems.

Abbas et al. [26] have noticed heat transfer coefficient and Nusselt number increase of 26.7% and 20.03% at 0.009% volume concentration of 50:50% of Fe_2O_3-TiO_2/water hybrid nanofluid flow in a car radiator. Krishna et al. [27] observed a maximum enhancement in Nusselt number of 3% of hybrid MWCNT-CuO/water nanofluid rather than the individual CuO/water and MWCNT/water mono-nanofluids. Iftikhar et al. [28] have noticed the higher heat transfer coefficient for Cu–SiO_2/water hybrid nanofluid as compared to Cu-water/nanofluid. Sundar et al. [29] found that the Nusselt number enhancement of 0.3% volume concentration of ND-Ni/water hybrid nanofluid is 35.43% with a friction factor penalty of 1.12 times at a Reynolds number of 22,000 compared to distilled water. Sundar et al. [30] also observed Nusselt number increase of 31.1% with a friction factor penalty of 1.18 times of 0.3% volume concentration of MWCNT-Fe_3O_4/water hybrid nanofluid at a Reynolds number of 22,000 over the water data. Gupta et al. [31] found increased heat transfer coefficient for zinc ferrite/water hybrid nanofluid flow in a tube. The earlier research work shows that hybrid nanofluids offer higher heat transfer coefficient rather than the single nanoparticles-based nanofluids as well as base fluid.

Apart from the heat transfer augmentation with hybrid nanofluids, some researchers have analyzed the second law efficiency of hybrid nanofluids. Saleh and Sundar [32] noticed the exergy efficiency enhancement of 42.27% at 0.6% of Ni/water nanofluid flow in a plate heat exchanger at a Reynolds number of 707. Saleh and Sundar [33] also observed exergy efficiency increase of 17.54% at 0.2% of ND + Fe_3O_4/60% ethylene glycol and 40% water hybrid nanofluid flow in a tube at a Reynolds number of 7218. Kumar et al. [34] have investigated exergy analysis of water-based Al_2O_3 + MWCNT, TiO_2 + MWCNT, ZnO + MWCNT and CeO_2 + MWCNT hybrid nanofluids flow in a plate heat exchanger and observed among all the hybrid nanofluids; the CeO_2 + MWCNT offers higher exergetic performance. Dezfulizadeh et al. [35] have observed 7% increase of exergy efficiency for water-based Cu–SiO_2–MWCNT ternary hybrid nanofluid in a heat exchanger at a Reynolds number of 12,000. The researchers have observed that the exergy efficiency is higher for hybrid nanofluids compared to base fluid.

The heat transfer coefficient of hybrid nanofluids may further be enhanced by creating the flow turbulence. The flow turbulence may be created by using some kind of inserts. The inserts may be twisted tape [36], longitudinal strip [37], helical coil [38], coiled wire [39], etc. Among all the inserts, the coil wire inserts are simple in construction and easy to operate with a negligible friction factor and pressure drop [40]. The literature related to hybrid nanofluids with coiled wire inserts is presented below. Hamid et al. [41] have observed thermal performance factor improvement up to 2.06 at $\phi = 2.5\%$ of TiO_2–SiO_2 hybrid nanofluid and with coiled wire insert of p/d of 1.50. Azmi et al. [42] noticed thermal performance factor improvement of 1.72 at $\phi = 1.0\%$ of 0.2 composition ratio of TiO_2–SiO_2 hybrid nanofluid and with coiled wire insert of p/d of 0.83. Kumar and Sarkar [43] have studied the thermal performance analysis using Al_2O_3 + MgO hybrid nanofluid and with coiled wire configurations of converging, diverging and converging–diverging type and noticed higher thermal performance of 1.69 for coiled wire configuration of diverging type compared to other type configurations. Shahsavar et al. [44] observed that the overall hydrothermal performance of twisted tape inserted double-pipe heat exchanger contains a higher value of 2.671 at a Reynolds number of 2000 and volume concentration of 3% and twisted tape pitch of 4 mm. Shahsavar et al. [45] have observed that the Nusselt number increase of 30% at ϕ is equal to 1% of Ag–water nanofluid and also they observed thermal and frictional entropy generation rates that reached up to 30.25% and 77.60% with same particle loadings in the finless annulus. Yıldız et al. [46] have studied numerically about the natural convective heat transfer of flow of fluid over an enclosure and observed Nusselt number increase of 25% using the dome shape enclosure instead of rectangular or square enclosure. Hussain et al. [47] numerically studied the heat transfer of mixed convection of Al_2O_3–Cu–water hybrid nanofluid in a wavy channel with a circular cylinder based on the Galerkin finite element method and observed heat transfer enhancement by 200%.

Ghachem et al. [48] numerically studied the heat transfer coefficient of CNT–Al_2O_3–water hybrid nanofluid flow in a cross flow micro heat exchanger and observed higher heat transfer coefficients.

The present research work aims to analyze experimentally about the second (exergy) law efficiency, thermal entropy generation, frictional entropy generation, heat transfer coefficient and friction factor of hybrid nanofluids flow in a tube and with a coiled wire inserts, which is not available in the open literature. For this purpose, the present study is undertaken to analyze those thermodynamics concepts of hybrid nanofluids flow in a tube with coiled wire inserts. The water-based nanodiamond + Fe_3O_4 nanofluids are prepared and used for the analysis. Additionally, the Nusselt number and pressure drop are also studied experimentally at different particle loadings of 0.05%, 0.1% and 0.2% and coiled wire inserts of pitch/diameter (p/d) ratio of 3.67, 2.34 and 1.00. The experiments were undertaken in the Reynolds number range from 2000 to 20,000.

Formulation

The problem is formulated to analyze the second law of thermodynamics exergy efficiency and entropy generation of ND + Fe_3O_4 nanofluid flow in a tube and with coiled wire inserts. The below-mentioned mathematical expressions are considered. Initially, the fluid inlet, outlet and wall temperatures are measured experimentally and substituted in the expressions to estimate the Nusselt number followed by heat transfer coefficient and those are considered for the second law efficiency analysis.

Second law (exergy) efficiency and thermal entropy generation

The heat supplied (Q_h) to the test tube [49] and heat absorbed by the fluid $\left(Q_a\right)$ [49] are analyzed from Eqs. (1) and (2). Equations (7) and (8) are considered for thermal entropy generation [50] and exergy efficiency [51] analysis.

(a) Rate of heat supplied to the test tube, $Q_h = V \cdot I$ (1)

(b) Rate of heat absorbed by the fluid, $Q_a = \dot{m} \cdot C_p \cdot \left(T_o - T_i\right)$ (2)

(c) Average heat transfer rate, $Q_{avg} = \dfrac{\left(Q_h + Q_a\right)}{2}$ (3)

(d) Heat transfer coefficient, $h = \dfrac{Q_{avg}}{A\left(T_s - T_m\right)}$ (4)

where $A = \pi \cdot D \cdot L; T_s = \frac{T_1+T_2+T_3+T_4+T_5}{5}; T_m = \frac{T_o+T_i}{2}$.

Heat transfer coefficient from Eq. (4) is substituted in Eq. (5) for the Nusselt number evaluation.

(e) Nusselt number,

$$Nu = \frac{h \cdot D}{k} \tag{5}$$

(f) Prandtl number,

$$Pr = \frac{\mu \cdot C_P}{k} \tag{6}$$

(g) Thermal entropy generation,

$$\dot{S}_{g,H} = \frac{Q_{avg}^2}{Nu \cdot \pi \cdot k \cdot T_{in} \cdot T_{out} \cdot L} \tag{7}$$

(h) Exergy efficiency,

$$\eta_{ex} = 1 - \frac{T_a \cdot \dot{S}_{g,H}}{\left[1 - \left(\frac{T_a}{T_s}\right)\right] Q_{ag}} \tag{8}$$

Entropy generation number

In order to evaluate the irreversibility loss in the tube, Bejan [52] redefined the entropy generation number as,

$$Ns = \frac{\dot{S}_{gen,H}}{\dot{m} \cdot C_p} \tag{9}$$

and Bejan indicated that the smaller the entropy generation number, the better the performance of the tube.

In order to clear up the physical interpretation of Bejan's entropy generation number multiplying both the numerator and denominator by ΔT_{min} (the temperature rise or drop of the fluid with the smaller heat capacity rate) yields,

$$Ns = \frac{\dot{S}_{gen,H} \Delta T_c}{\dot{m} C_p \Delta T_c} = \frac{\dot{S}_{gen,H}}{Q_{avg}} \tag{10}$$

Frictional entropy generation

Equation (11) estimates the frictional entropy generation [50].

(i) Frictional entropy generation,

$$\dot{S}_{g,F} = \frac{8 \cdot f \cdot \dot{m}^3 \cdot L}{\rho^2 \cdot \pi^2 \cdot D_i^5 \cdot (T_o - T_i)} \cdot \ln\left(\frac{T_o}{T_i}\right) \quad (11)$$

Equations (12) and (13) estimate the pressure drop [53] and friction factor [49].

(j) Pressure drop,

$$\Delta P = \rho_{nf} \cdot g \cdot H \quad (12)$$

(k) Friction factor,

$$f = \frac{(\Delta P)}{\left(\frac{L}{D}\right) \cdot \left(\frac{\rho v^2}{2}\right)} \quad (13)$$

where $\dot{m} = \rho \cdot A \cdot v \Rightarrow v = \frac{\dot{m}}{\rho \cdot A}$.

The pressure drop [53] from Eq. (12) is substituted in Eq. (14) for the evaluation of pumping power [53].

(xii) Pumping power,

$$Pp = \left(\frac{\dot{m}}{\rho_{nf}}\right) \cdot \Delta P \quad (14)$$

Total entropy generation and Bejan number

Equations (15) and (16) estimate the total entropy generation [50] and Bejan number [52].

(xiii) Total entropy generation,

$$\dot{S}_g = \dot{S}_{g,H} + \dot{S}_{g,F} \quad (15)$$

(xiv) Bejan number,

$$Be = \frac{\dot{S}_{g,H}}{\dot{S}_{g,H} + \dot{S}_{g,F}} \quad (16)$$

Experimental

Preparation of hybrid nanofluid

The hybrid nanoparticles were selected based on the high thermal conductivity and high magnetic properties. Among all the materials, the nanodiamond (ND) particles offer high thermal conductivity property; in the same way, among all the materials, magnetite (Fe_3O_4) offers high magnetic properties. By combining these two materials, the hybrid nanoparticle of ND + Fe_3O_4 offers synergistic property of both high thermal conductivity and high magnetic property.

Table 1 The physical property of water, ND, Fe_3O_4 and ND + Fe_3O_4 nanoparticles

Substance	ρ/kg m^{-3}	k/W m^{-1} K^{-1}	C_p/J kg^{-1} K^{-1}	μ/mPa.s
Water	998.5	0.602	4178	0.89
ND	3100	1000	516	–
Fe_3O_4	5810	80.1	670	–
ND + Fe_3O_4	5051.2	337.74	628.88	–

Such type of magnetic nanoparticles is used in micro-fluidics, drug delivery, etc. The detailed explanation for the synthesis of dry hybrid nanoparticles given by Sundar et al. [54] is used. The physical property of water, ND, Fe_3O_4 and ND + Fe_3O_4 nanoparticles is indicated in Table 1. For the exergy efficiency, heat transfer, entropy generation analysis water-based ND + Fe_3O_4 hybrid nanofluids were prepared at 0.05%, 0.1% and 0.2% particle volume concentrations. The hybrid nanoparticles used in this work have been synthesized based on the Sundar et al. [54] method. Since the nanoparticles are synthesized in the laboratory, the upper limit of the nanoparticle loadings was fixed to 0.2% volume concentration.

A total of 18 L hybrid nanofluid was prepared by dispersing 45.59, 91.18 and 182.36 g of dry ND + Fe_3O_4 hybrid nanoparticles in the distilled water in the particle volume concentrations of 0.05%, 0.1% and 0.2% and then stirred with mechanical stirrer at low rpm. The thermophysical properties of Sundar et al. [54] have been used and its values are given in Table 2.

Forced convection apparatus

The forced convection apparatus is fabricated and its line diagram is indicated in Fig. 1a. The copper tube with an inner diameter (D) of 0.019 m, outer diameter (D_o) of 0.021 m and length (L) of 1.7 m was used, in which at 0.1875, 0.375, 0.750, 1.125 and 1.312 m distance from left-side of the tube, five J-type thermocouples are placed to measure the tube surface temperatures. Another two J-type thermocouples are also used to measure the fluid inlet and outlet temperatures with an accuracy of ± 0.1 °C. Constant heat flux boundary condition is maintained with nichrome heating element coil of 0.812 mm diameter with a resistance of 0.193487 Ωm and 2000 W. The asbestos rope is used to insulate the test section. The fluid flow in the test tube was maintained by means of pump with an accuracy of ± 0.1 kg/s. Based on the defined Reynolds number, the mass flow rate of base fluid and nanofluid is adjusted and allowed into the test tube. The excess fluid is sent back to the receiving tank by using bypass valve arrangement. The

Table 2 Thermophysical properties of hybrid nanofluids

Thermophysical properties of ND + Fe_3O_4 hybrid nanofluids				
k/W $m^{-1}K^{-1}$	$\phi=0.0\%$	$\phi=0.05\%$	$\phi=0.1\%$	$\phi=0.2\%$
20	0.602	0.615	0.634	0.657
30	0.616	0.636	0.659	0.687
40	0.631	0.648	0.670	0.703
50	0.642	0.676	0.693	0.736
60	0.653	0.684	0.717	0.769
ρ/kg m^{-3}				
20	997	999.03	1001.05	1005.11
30	997.5	999.53	1001.55	1005.61
40	995	997.03	999.06	1003.11
50	990	992.03	994.06	998.12
60	985	987.03	989.07	993.13
C_p/J kg^{-1} K^{-1}				
20	4178	4176.22	4174.45	4170.9
30	4178	4176.22	4174.45	4170.9
40	4179	4177.22	4175.45	4171.9
50	4180.5	4178.72	4176.95	4173.39
60	4183	4181.22	4179.44	4175.89
μ/mPa s				
20	1.006	1.5281	1.5663	1.6045
30	0.831	1.0752	1.1498	1.2257
40	0.657	0.7939	0.8377	0.8828
50	0.567	0.7945	0.8607	0.9269
60	0.478	0.7369	0.7807	0.8265

outlet temperature of the test fluid is reduced to atmospheric temperature using water chiller.

For water, 0.05%, 0.1% and 0.2% volume concentration of nanofluids flow in a tube, the used Reynolds number range for this study is as follows: 2756 to 21,820 (water); 2649 to 21,678 ($\phi=0.05\%$); 2574 to 20,886 ($\phi=0.1\%$); and 2516 to 20,095 ($\phi=0.2\%$), respectively. Based on the Reynolds number, the mass flow rate is adjusted. Based on the pump capacity, the mass flow rates are fixed; accordingly, the Reynolds number is calculated.

The heat supplied to the test tube is 1100 W ($220V \times 5A$). The temperature readings were noted down when the system reached to steady state. The system takes 2 h for reaching the steady state.

Coiled wire inserts

The fluid turbulence is provided by using coiled wire inserts inside the tube. The analysis of exergy and entropy generation was studied further at different pitch (p) to diameter (d) ratio of coiled wire inserts. The line diagram of Fig. 1b indicates the coiled wire insert inside a tube. The thickness of 2 mm wire of spring steel is turned like a coiled wire of pitches (p), i.e., 19, 44.46 and 69.73 mm. Hydraulic diameter (Eq. 17) is used to calculated the Reynolds number for coiled wire inserts. The calculated hydraulic diameter is noted in Table 3.

Hydraulic diameter [55],

$$d_h = \frac{4A}{p} \Rightarrow d_h = \frac{4\left[\frac{\pi d_i^2}{4} - \frac{\pi t^2\left(\frac{d_i}{p}\right)}{4}\right]}{\left[\pi d_i + \pi t\left(\frac{d_i}{p}\right)\right]} \tag{17}$$

Results and discussion

Bench mark analysis

Nusselt number

The obtained heat transfer coefficient (h) from Eq. (4) is converted into non-dimensional Nusselt number from Eq. (5). First, the water heat transfer coefficient is converted into Nusselt number and compared with the Gnielinski [56] data. Figure 2a is the comparison between experimental and theoretical Nusselt number, and it is found a maximum of ± 3% deviation.

Gnielinski [56],

$$Nu = \frac{\left(\frac{f}{2}\right)(Re - 1000)\,\mathrm{Pr}}{1.07 + 12.7\left(\frac{f}{2}\right)^{0.5}\left(\mathrm{Pr}^{2/3} - 1\right)} \tag{18}$$

$$f = (1.58\ln(Re) - 3.82)^{-2}$$

$$0.5 < \mathrm{Pr} < 2000; 2300 < Re < 10^6$$

Friction factor

The estimated pressure drop from Eq. (12) is converted into non-dimensional parameter of friction factor based on Eq. (13) for water and the data is noted in Fig. 2b with Eq. (19) data. From the figure, it is found to be a maximum of ± 2.5% between experimental and theoretical friction factor.

(i) Blasius [57],

$$f = 0.3164Re^{-0.25} \tag{19}$$

$$3000 < Re < 10^5$$

Temperature difference $(T_s - T_m)$ of hybrid nanofluids and coiled wire inserts

The difference between surface and mean temperatures of the fluid for water, 0.05%, 0.1% and 0.2% vol. nanofluids at various Reynolds number (Re) and p/d were analyzed first. The raw temperature data are used for heat transfer coefficient, Nusselt number and thermal entropy generation

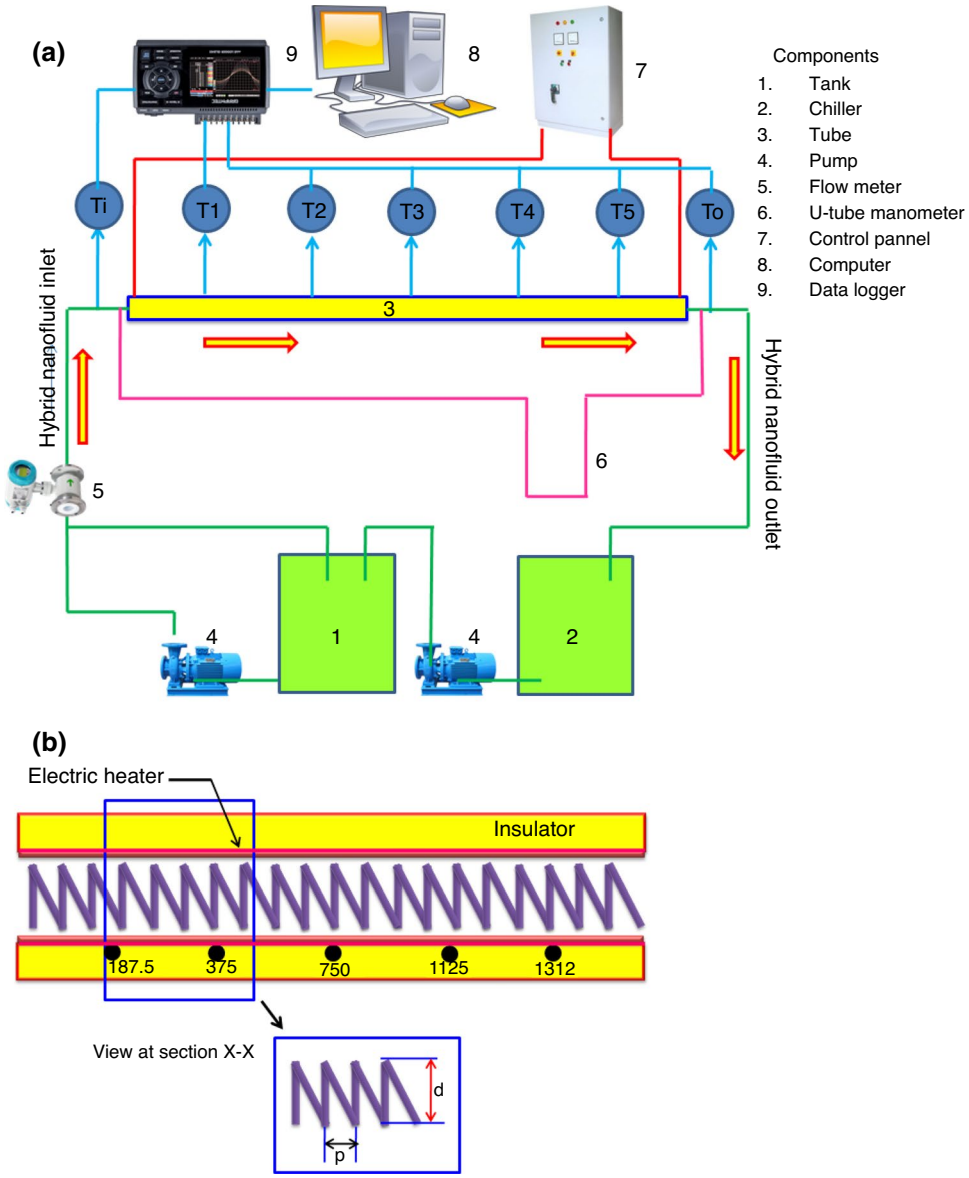

Fig. 1 **a** The schematic representation of an experimental test facility, and **b** coiled wire inserts in a test tube

Table 3 Dimensions of the coiled wire inserts (dimensions are in mm)

Diameter/D/mm	Pitch/p/mm	Pitch/diameter/p/D	Hydraulic diameter, d_h/mm
19	19.00	1.00	17.00
19	44.46	2.34	18.09
19	69.73	3.67	18.41
19	(Plain tube without insert)		

calculations. Figure 3a indicates the $(T_s - T_m)$ data of water flow in a tube and with various p/d values under different Reynolds numbers. From the figure, it is understandable that, at the lower *Re* values, the temperature difference is more, but when the *Re* value is increased, the temperature difference is lesser. For water in a plain tube, the temperature difference values are 16.98 °C and 2.07 °C at Reynolds number of 2756 and 21,820. Under the same Reynolds numbers, for water in a tube with p/d of 3.67, the temperature difference values are 15.93 °C and 1.81 °C. Moreover, at same Reynolds numbers, for water in a tube with p/d of 2.34, the temperature difference values are 15.45 °C and 1.71 °C. Similarly, under same Reynolds numbers, for water in a tube with p/d of 1.00, the temperature difference values are 14.26 °C and 1.56 °C, respectively.

The similar nature of decreased temperature difference was noticed for nanofluids as well as with an increase of *Re* and decrease of p/d values. Figure 3b indicates the $T_s - T_m$ values of 0.05% vol. and with different p/d and *Re* values. At Reynolds numbers of 2649 and 21,678, the temperature

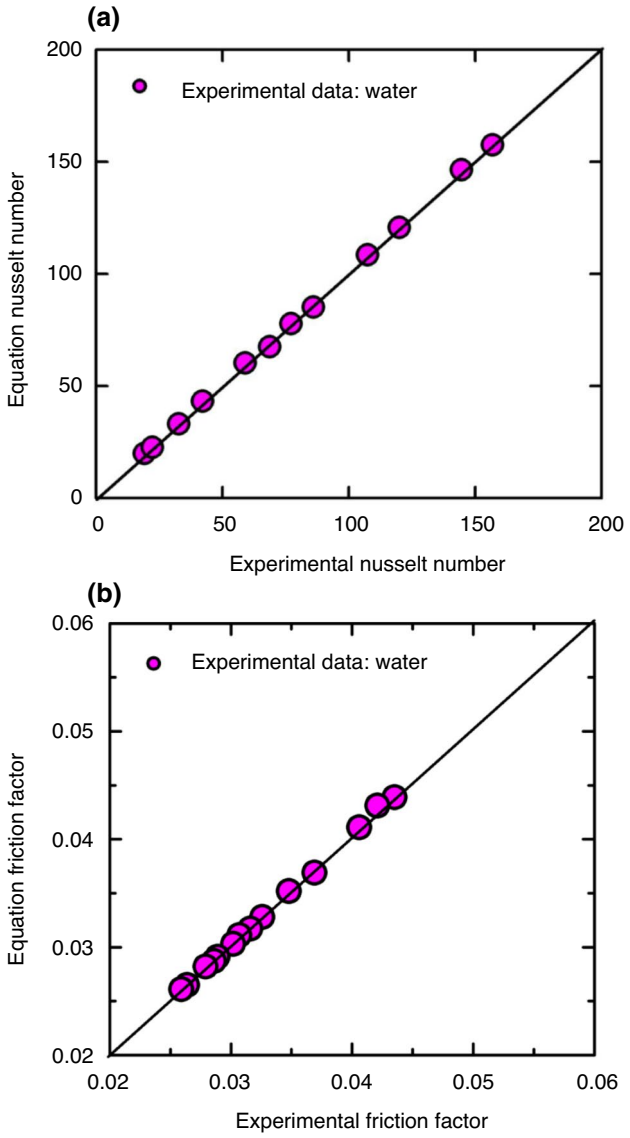

Fig. 2 **a** Validation of experimental Nusselt number of water with Eq. (18) data. **b** Validation of experimental friction factor of water with Eq. (19) data

difference of $\phi = 0.05\%$ hybrid nanofluid is 15.74 °C and 1.68 °C; the temperature difference of $\phi = 0.05\%$ hybrid nanofluid in a tube with p/d of 3.67 is 14.35 °C and 1.42 °C; the temperature difference of $\phi = 0.05\%$ hybrid nanofluid in a tube with p/d of 2.34 is 13.94 °C and 1.35 °C; the temperature difference of $\phi = 0.05\%$ hybrid nanofluid in a tube with p/d of 1.00 is 12.72 °C and 1.24 °C, respectively.

Figure 3c depicts the $T_s - T_m$ of $\phi = 0.1\%$ hybrid nanofluid with different p/d and Re values. At $\phi = 0.1\%$ hybrid nanofluid in a tube without inserts, the temperature differences are 14.98 °C and 1.56 °C at Reynolds numbers of 2574 and 20,886. Under the same Reynolds number, for $\phi = 0.1\%$ hybrid nanofluid in a tube with p/d of 3.67 the temperature differences are 13.43 °C and 1.28 °C. Moreover for $\phi = 0.1\%$ hybrid nanofluid in a tube with p/d of 2.34, the temperature differences are 12.94 °C and 1.22 °C at same Reynolds numbers. Meanwhile for $\phi = 0.1\%$ hybrid nanofluid in a tube with p/d of 1.00, the temperature differences are 11.82 °C and 1.12 °C at same Re values, respectively.

Figure 3d shows the $T_s - T_m$ of $\phi = 0.2\%$ hybrid nanofluid with various p/d and Re values. At constant Reynolds numbers of 2516 and 20,095, the temperature difference of $\phi = 0.2\%$ hybrid nanofluid in a plain tube is 14.02 °C and 1.43 °C; temperature difference of $\phi = 0.2\%$ hybrid nanofluid in a plain tube with p/d of 3.67 is 12.29 °C and 1.15 °C; temperature difference of $\phi = 0.2\%$ hybrid nanofluid in a plain tube with p/d of 2.34 is 11.69 °C and 1.1 °C; temperature difference of $\phi = 0.2\%$ hybrid nanofluid in a plain tube with p/d of 1.00 is 10.87 °C and 1.00 °C, respectively.

Equation (4) evaluates the heat transfer coefficient, and those values depend on Q_{avg}, area (A) and the temperature difference $(T_s - T_m)$. The temperature difference $(T_s - T_m)$ in Eq. (3) is inversely proportional to heat transfer coefficient. The constant amount (Q_h) of 1100 W was applied to the test tube for all the experiments. The area, $A = \pi DL$; here for the plain tube without inserts, the D is considered as 0.019 m, and for plain tube with coiled wire inserts p/d of 3.67, 2.34 and 1.00, the D is considered as 0.0184, 0.01809 and 0.017 m, which is the hydraulic diameter (D_h). Hence, the calculated area for plain tube is 0.1014 m^2; the calculated area for plain tube with p/d of 3.67, 2.34 and 1.00 is 0.09821, 0.0965, 0.0907 m^2, respectively. Hence for the fixed average rate of heat flow (Q_{avg}) and area (A), the heat transfer coefficient depends on $T_s - T_m$. The decrease in $T_s - T_m$ value indicates the increase in heat transfer coefficient. From the experimental temperature difference values, it is observed that the coiled wire insert of $p/d = 1.00$ has the less $T_s - T_m$ value compared other coiled wire inserts inside the tube. Hence, it is expected that the higher heat transfer coefficients for the coiled wire insert $p/d = 1.00$ compared to other type of inserts.

Heat transfer coefficient of hybrid nanofluids and with coiled wire inserts

The experimentally obtained $T_s - T_m$ values were used in Eq. (4) to evaluate the experimental heat transfer coefficient (h) for water and nanofluids and with coiled wire inserts. Figure 4a indicates the heat transfer coefficient of water flow in a tube with and without coiled wire inserts at various Reynolds numbers. Figure shows that the h is increased with an increase in Re and decrease in coiled wire p/d values. When water in a tube with $p/d = 3.67$, the h is increased to 6.61% and 14.63% at Re equal to 2756 and 21,820, compared to water without inserts. However, for water in a tube with $p/d = 2.34$, the h is increased to 9.92% and 21.33% at same

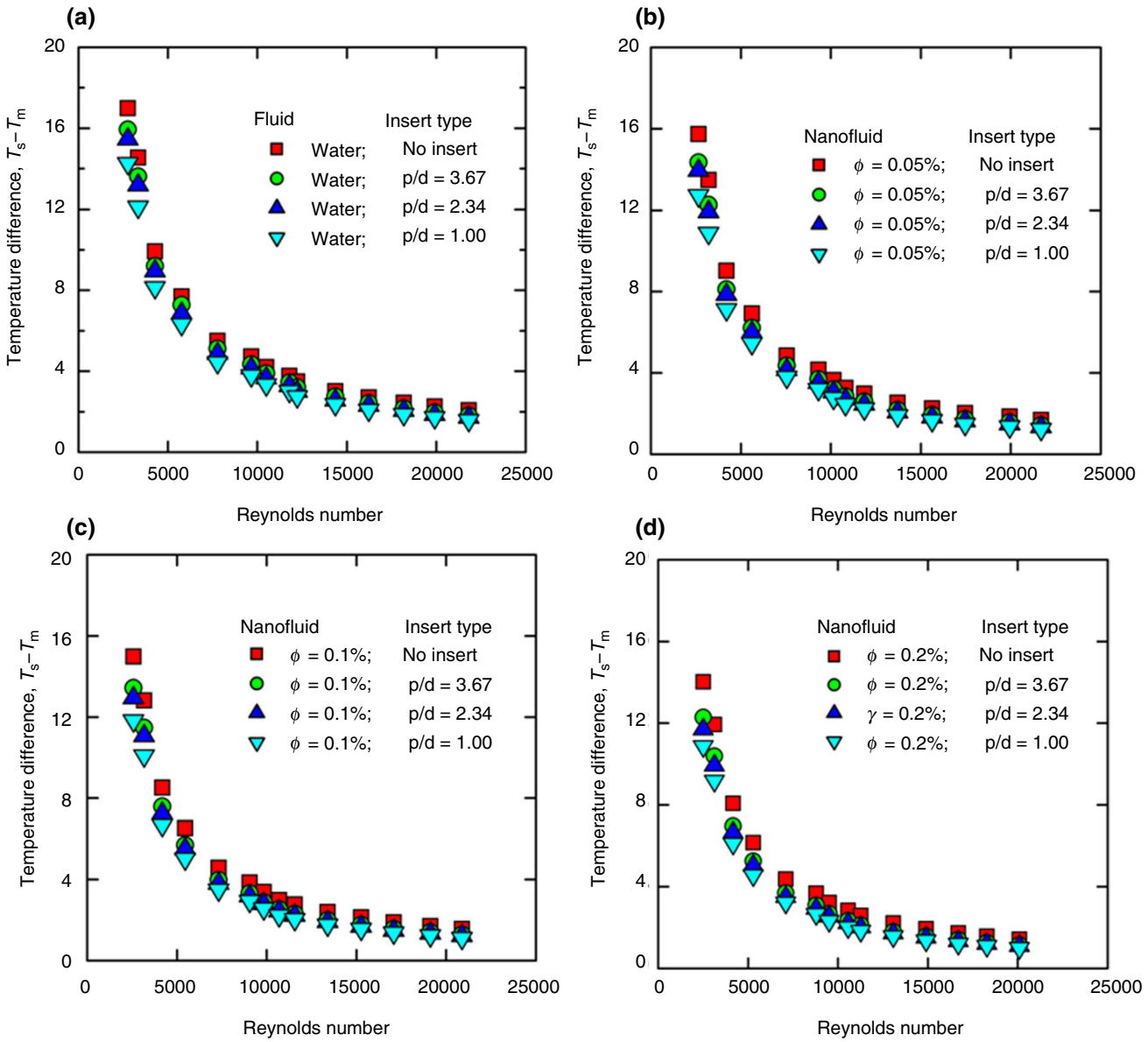

Fig. 3 Temperature difference with effect of Reynolds numbers, volume concentrations and coiled wire inserts for **a** water, **b** $\phi = 0.05\%$, **c** $\phi = 0.1\%$ and **d** $\phi = 0.2\%$ nanofluids

Reynolds numbers compared to water without insert. Moreover, for water in a tube with $p/d = 1.00$, the h is increased to 19.13% and 32.03% at same Reynolds numbers compared to water without inserts.

The heat transfer coefficient of $\phi = 0.05\%$ of nanofluid with various coiled wire inserts and Reynolds number is indicated in Fig. 4b. Noticed from the figure, the h is raised with rise in Re and lower of coiled wire p/d values. For $\phi = 0.05\%$ nanofluid in a plain tube with coiled wire insert of $p/d = 3.67$, the h is increased to 9.66% and 18.43% at Re of 2649 and 21,678 against the same nanofluid without insert. However, at $\phi = 0.05\%$ nanofluid with coiled wire insert of $p/d = 2.34$, the h is increased to 12.92% and 24.43% at same Reynolds number and same nanofluid without insert. Moreover, at $\phi = 0.05\%$ nanofluid in a plain tube with coiled wire insert of $p/d = 1.00$, the h is increased to 23.68% and 36.04% at same Reynolds number and same nanofluid without insert, respectively.

Similarly, the heat transfer coefficient of $\phi = 0.1\%$ nanofluid with different coiled wire inserts and Reynolds numbers is presented in Fig. 4c. The nature of h increases with increase in Re and decrease in coiled wire p/d is observed from the figure. For $\phi = 0.1\%$ nanofluid with p/d of 3.67, the h which is increased to 11.56% and 21.46% at Re is equal to 2574 and 20,886 against the same nanofluid without insert. However, at $\phi = 0.1\%$ nanofluid with p/d of 2.34, the h is

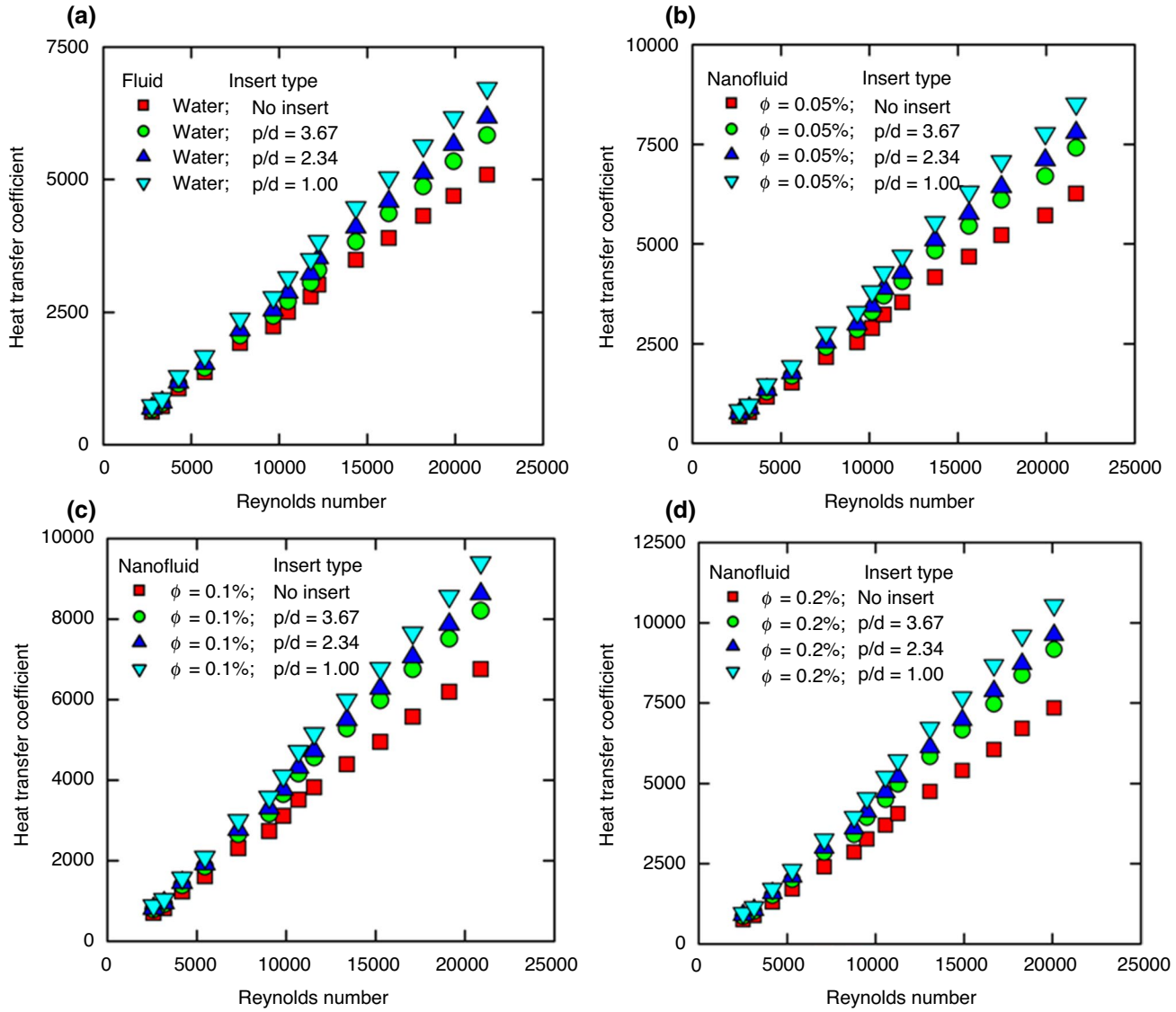

Fig. 4 Heat transfer coefficient with effect of Reynolds numbers, volume concentrations and coiled wire inserts for **a** water, **b** $\phi = 0.05\%$, **c** $\phi = 0.1\%$ and **d** $\phi = 0.2\%$ nanofluids

increased to 15.77% and 27.71% at same Reynolds number and same nanofluid without insert. Moreover, at $\phi = 0.1\%$ nanofluid with p/d of 1.00, the h is increased to 26.72% and 39.21% at same Reynolds number and same nanofluid without insert, respectively.

Figure 4d reveals the h values of $\phi = 0.2\%$ nanofluid flow with various p/d values under different Reynolds numbers. Figure shows that the h value is increased with an increase in Re and decrease in p/d values. For $\phi = 0.2\%$ nanofluid with p/d of 3.67, the h which is increased to 14.13% and 24.73% at Re is equal to 2516 and 20,095 against the same nanofluid without insert. However, at $\phi = 0.2\%$ nanofluid with p/d of 2.34, the h is increased to 19.99% and 30.88% at same Reynolds number and same nanofluid without insert. Moreover, at $\phi = 0.2\%$ nanofluid with p/d of 1.00, the h is increased to 28.98% and 43.52% at same Reynolds number and same nanofluid without inserts, respectively.

Nusselt number of hybrid nanofluids and with coiled wire inserts

Initially, water with different p/d values experiments was conducted. Later, the experiments were extended to nanofluids with different p/d values. For water and nanofluids with coiled wire inserts also, the same equations of (4) and (5) are used to estimate the heat transfer coefficient and Nusselt number. The Nusselt number of water with various p/d values is presented in Fig. 5a at different Reynolds numbers.

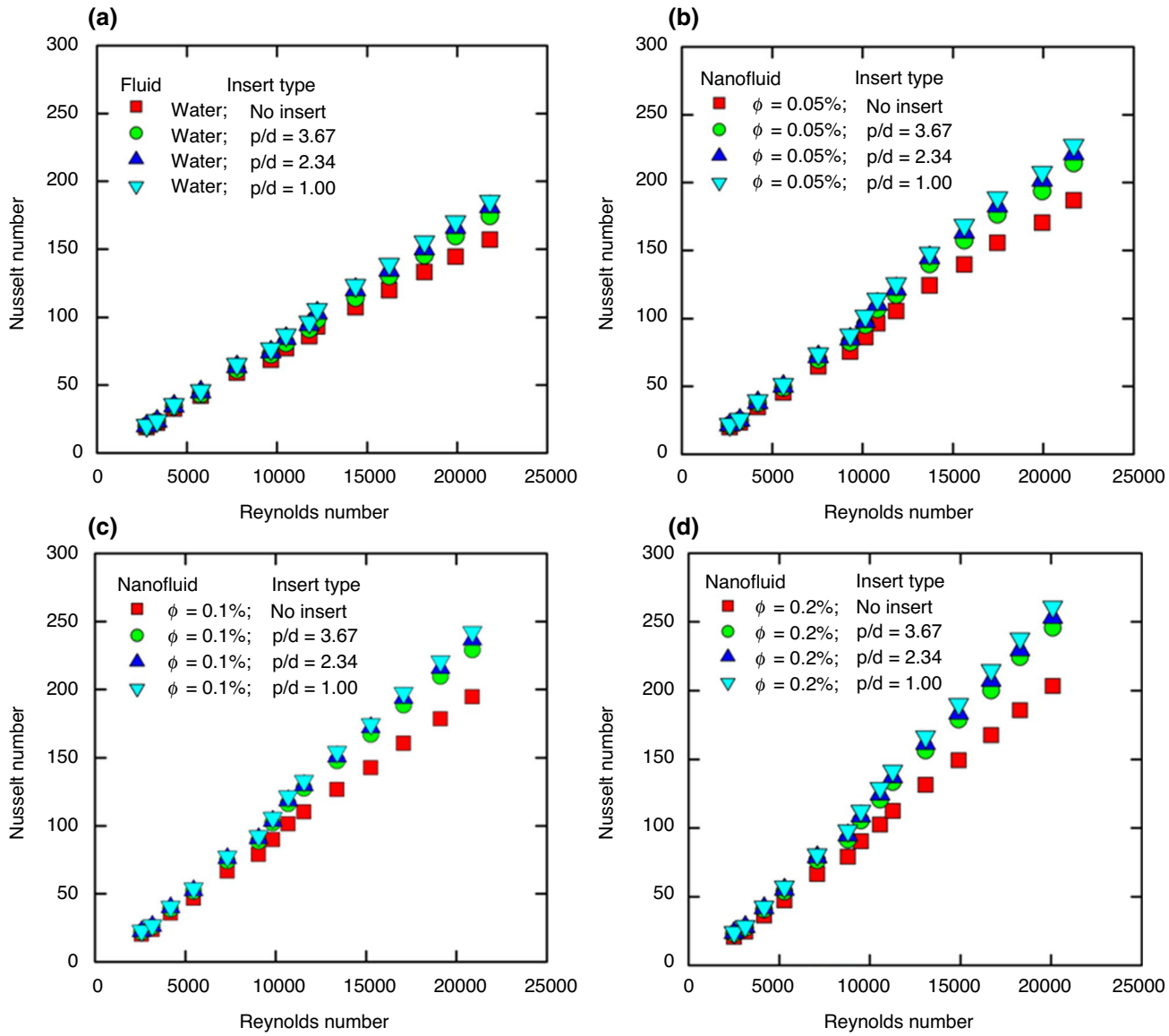

Fig. 5 Nusselt number with effect of Reynolds numbers, volume concentrations and coiled wire inserts for **a** water, **b** $\phi = 0.05\%$, **c** $\phi = 0.1\%$ and **d** $\phi = 0.2\%$ nanofluids

The Nusselt number is increased with an increase in Reynolds number and decrease in p/d values. Water in a tube with p/d of 3.67, the Nusselt number is increased to 3.29% and 11.07% at Reynolds number of 2756 and 21,820 against water without inserts. However, for water with p/d of 2.34, the Nu is increased to 4.65% and 15.52% at same Reynolds number and water without insert. Moreover, for water with p/d of 1.00, the Nu is increased to 6.59% and 18.14% at same Reynolds number and water without insert.

Figure 5b indicates the Nu of $\phi = 0.05\%$ nanofluid with various p/d and Re values. It is noticed that the Nu is increased with an increase in Re and decrease in p/d values. For $\phi = 0.05\%$ nanofluid with p/d of 3.67, the Nu is increased to 6.26% and 14.76% at Reynolds number of 2649 and 21,678 over the same nanofluid without insert. However, at $\phi = 0.05\%$ nanofluid with p/d of 2.34, the Nu is increased to 7.51% and 18.47% at same Reynolds number and same nanofluid without insert. Moreover, at $\phi = 0.05\%$ nanofluid with p/d of 1.00, the Nu is increased to 10.66% and 21.72% at same Reynolds number and same nanofluid without insert.

Figure 5c depicts the Nu of $\phi = 0.1\%$ nanofluid with different p/d and Re values. The Nu is increased with an increase in Re and decrease in p/d values. For $\phi = 0.1\%$ nanofluid with p/d of 3.67, the Nu is increased to 8.10% and 17.69% at Reynolds number of 2574 and 20,886, over the same nanofluid without insert. However, for $\phi = 0.1\%$ nanofluid with p/d of 2.34, the Nu is increased to 10.22% and 21.59% at same Reynolds number and same nanofluid

Table 4 The obtained Nusselt number values for water and $\phi = 0.05\%$ nanofluid

Re	Nusselt number for $\phi = 0\%$				Re	Nusselt number for $\phi = 0.05\%$			
	$\frac{p}{d_i}=0$	$\frac{p}{d_i}=3.67$	$\frac{p}{d_i}=2.34$	$\frac{p}{d_i}=1$		$\frac{p}{d_i}=0$	$\frac{p}{d_i}=3.67$	$\frac{p}{d_i}=2.34$	$\frac{p}{d_i}=1$
2756	19.12	19.75	20.01	20.38	2649	19.98	21.23	21.48	22.11
3339.14	22.34	23.12	23.45	23.98	3214	23.34	24.85	25.12	25.85
4282.88	32.71	34.21	34.56	35.65	4212	34.87	37.56	38.12	39.45
5763.86	42.18	43.23	44.98	45.98	5626	45.34	48.96	49.98	51.49
7778.17	59.06	61.45	63.45	65.45	7550	64.67	69.85	71.98	73.98
9665.82	68.7	72.45	74.53	76.76	9311	75.67	82.65	84.95	87.98
10,496.7	77.18	80.81	84.44	86.98	10,162	86.34	95.32	97.89	101.75
11,789.3	86.05	91.23	94.54	96.45	10,810	96.45	106.98	110.54	114.26
12,228.4	93.11	98.34	103.21	105.76	11,856	105.56	117.56	121.65	125.42
14,353.9	107.4	114.23	120.23	123.34	13,711	124.34	139.74	144.75	147.98
16,233.2	119.96	130.21	134.45	138.87	15,635	139.56	157.45	163.47	168.47
18,184.4	132.97	145.34	150.32	155.43	17,469	155.67	176.48	182.64	188.75
19,918.4	144.55	159.54	165.98	170.21	19,949	170.34	193.64	201.68	207.54
21,820.4	156.87	174.23	181.21	185.32	21,678	186.76	214.32	221.25	227.32

without insert. Moreover, for $\phi = 0.1\%$ nanofluid with p/d of 1.00, the Nu is increased to 13.38% and 24.56% at same Reynolds number and same Nanofluid without inserts.

Figure 5d understands the Nu of $\phi = 0.2\%$ nanofluid with various p/d and Re values. It is found that the Nu is increased with an increase in Re and decrease in p/d values. For $\phi = 0.2\%$ nanofluid with p/d of 3.67, the Nu is increased to 10.59% and 20.86% at Reynolds number of 2516 and 20,095, over the same nanofluid without insert. However, at $\phi = 0.2\%$ nanofluid with p/d of 2.34, the Nu is increased to 14.24% and 24.61% at same Reynolds number and same nanofluid without insert. Moreover, at $\phi = 0.2\%$ nanofluid with p/d of 1.00, the Nu is increased to 15.40% and 28.42% at same Reynolds number and same nanofluid without insert. The particle migration and Brownian motion cause the increased Nusselt number of hybrid nanofluids [29]. The obtained Nusselt number values for water, 0.05%, 0.1% and 0.2% vol. of nanofluid are indicated in Tables 4 and 5.

Figure 6 indicates the comparison of experimental Nusselt number of ND + Fe_3O_4 nanofluid with coiled wire inserts with Hamid et al. [41] of TiO_2-SiO_2/60:40% EG/W nanofluid and Sundar et al. [58] of Fe_3O_4/water nanofluid. Decreasing p/d value from 3.67 to 1.00, the Nusselt number is increased, and the similar behavior has been observed by [41] and [58]. Sundar et al. [58] used Fe_3O_4/water nanofluids in a double-pipe heat exchanger with coiled wire inserts of 1.00, 1.34 and 1.79. The present data of ND + Fe_3O_4/water nanofluids with coiled wire inserts predict higher Nusselt number values compared to the Sundar et al. [58] of Fe_3O_4/

Table 5 The obtained Nusselt number values for $\phi = 0.1\%$ and $\phi = 0.2\%$ nanofluid

Re	Nusselt number for $\phi = 0.1\%$				Re	Nusselt number for $\phi = 0.2\%$			
	$\frac{p}{d_i}=0$	$\frac{p}{d_i}=3.67$	$\frac{p}{d_i}=2.34$	$\frac{p}{d_i}=1$		$\frac{p}{d_i}=0$	$\frac{p}{d_i}=3.67$	$\frac{p}{d_i}=2.34$	$\frac{p}{d_i}=1$
2574	20.25	21.89	22.32	22.96	2516	20.78	22.98	23.74	23.98
3169	23.67	25.63	26.12	26.89	3125	24.43	27.21	27.98	28.42
4193	35.65	38.74	39.87	40.65	4174	36.12	40.56	41.65	42.65
5457	46.54	51.65	52.48	53.98	5289	47.34	53.65	55.21	57.12
7325	66.45	74.12	76.12	77.48	7100	66.56	76.48	78.94	80.69
9048	78.87	88.47	90.64	92.47	8786	79.12	91.36	94.78	97.98
9840	89.78	101.95	103.45	105.94	9518	90.45	105.48	108.64	112.47
10,689	101.34	116.12	118.47	121.68	10,568	102.43	120.65	124.56	128.95
11,563	110.12	127.48	129.65	132.98	11,271	112.34	133.46	137.21	141.67
13,398	126.55	147.59	150.74	154.36	13,085	131.34	156.47	161.47	166.45
15,272	142.67	166.98	171.95	174.54	14,909	149.34	178.64	183.42	189.96
17,079	160.34	188.47	193.48	197.42	16,690	167.56	199.98	207.21	214.74
19,113	178.34	209.65	215.64	220.74	18,278	185.67	224.12	229.46	237.65
20,886	194.54	228.95	236.54	242.32	20,095	203.23	245.62	253.24	260.98

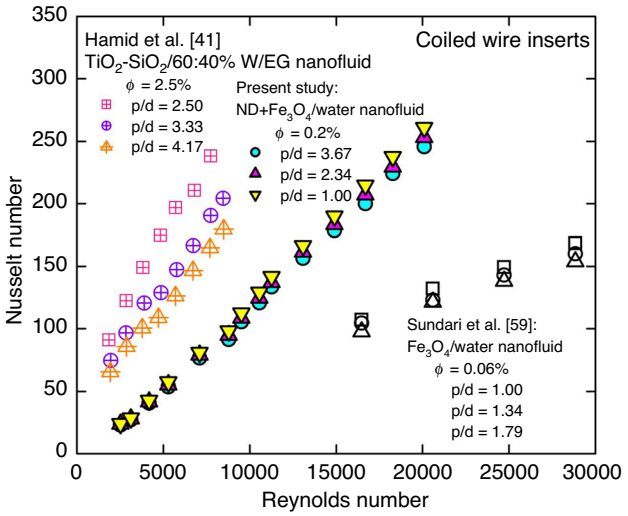

Fig. 6 Comparison of experimental Nusselt number of ND + Fe_3O_4 nanofluid with coiled wire inserts with Hamid et al. [41] of TiO_2-SiO_2/60:40% EG/W nanofluid and Sundar et al. [58] of Fe_3O_4/water nanofluid

water nanofluids with coiled wire inserts. This is caused because of the use of hybrid nanofluids in the present study. Hamid et al. [41] used TiO_2-SiO_2/60:40% EG/W nanofluids in a tube with coiled wire inserts. The present data predict lower values than the Hamid et al. [41] data, because of the different type of hybrid nanoparticles and the base fluids. The type of nanoparticles and base fluid also influence the Nusselt number of nanofluid.

The least value of the coiled wire pitch ratio represents the larger number of coils at a constant length. Therefore, more turbulence was generated by a large number of coils. Furthermore, the wire coil inserts will cause the redevelopment of thermal and hydrodynamic boundary layers. The similar ascending pattern of Nusselt number with decrease in coiled pitch to diameter ratio was observed in previous studies [59, 60].

Thermal entropy generation of hybrid nanofluids and with coiled wire inserts

Equation (7) evaluates the thermal entropy generation ($\dot{S}_{g,H}$) of the system. The Q_h supplied to the test tube is 1100 W. By substituting the temperatures, Nusselt number and thermal conductivity in Eq. (7), thermal entropy generation is estimated. The $\dot{S}_{g,H}$ for water and nanofluids in a tube and with coiled wire inserts was analyzed.

The obtained values of thermal entropy generation are shown in Fig. 7a at different p/d and Re values. As it is observed, the thermal entropy generation is decreased with an increase in Reynolds number and decrease in p/d values. Water with p/d of 3.67, the $\dot{S}_{g,H}$ which is decreased to 3.46% and 10.15% at Re is equal to 2756 and 21,820 against water without insert. However, for the water with p/d of 2.34 and p/d of 1.00, the $\dot{S}_{g,H}$ is decreased to 4.82% and 13.67%, and 6.98% and 15.77% at the same Reynolds number against to water without insert.

Figure 7b shows the $\dot{S}_{g,H}$ values of $\phi = 0.05\%$ nanofluid with various p/d and Re values. For $\phi = 0.05\%$ nanofluid with p/d of 3.67, the $\dot{S}_{g,H}$ is decreased to 6.27% and 13.05%, for p/d of 2.34, the $\dot{S}_{g,H}$ is decreased to 7.47% and 15.84%, and for p/d of 1.00, the $\dot{S}_{g,H}$ is decreased to 10.53% and 18.27% at Reynolds number of 2649 and 21,678 against the same nanofluid without insert.

Similarly, the thermal entropy generation of 0.1% nanofluid is shown in Fig. 7c along with various p/d and Re values. For $\phi = 0.1\%$ nanofluid with p/d of 3.67, the $\dot{S}_{g,H}$ is decreased to 8.03% and 15.24%, for p/d of 2.34, the $\dot{S}_{g,H}$ is decreased to 9.90% and 18.02%, and for p/d of 1.00, the $\dot{S}_{g,H}$ is decreased to 12.83% and 20.15% at Reynolds number of 2574 and 20,886 against the same nanofluid without insert.

Moreover, the thermal entropy generation of 0.1% nanofluid is shown in Fig. 7d along with various p/d and Re values. For $\phi = 0.2\%$ nanofluid with p/d of 3.67, the $\dot{S}_{g,H}$ is decreased to 10.20% and 17.47%, for p/d of 2.34, the $\dot{S}_{g,H}$ is decreased to 13.18% and 20.02%, and for p/d of 1.00, the $\dot{S}_{g,H}$ is decreased to 14.46% and 22.56% at Reynolds number of 2516 and 20,095 over the same nanofluid without insert.

With the decrease in p/d value of coiled wire insert, the effective fluid turbulence takes place in the test tube resulting that decreased thermal entropy generation; this behavior was noticed for all the fluids.

Frictional entropy generation of hybrid nanofluids and with coiled wire inserts

Equation (11) evaluates the frictional entropy generation ($\dot{S}_{g,F}$) of the system. Based on the friction factor, mass flow rate and temperatures, the frictional entropy generation is estimated. It is also further estimated for water and nanofluids in a tube and with coiled wire inserts.

Figure 8a indicates the $\dot{S}_{g,F}$ values of water flow in a tube and with various p/d and Re values. As it is noticed, the $\dot{S}_{g,F}$ is increased with an increase in Re and decrease in p/d values. For water with p/d of 3.67, the $\dot{S}_{g,F}$ which is decreased to 13.66% and 17.04% at Re is equal to 2756 and 21,820 against water without insert. However, for the water with p/d of 2.34, the $\dot{S}_{g,F}$ which is increased to 20.18% and 25.43% at Re is equal to 2756 and 21,820 against water without insert. Moreover, for the water with p/d of 1.00, the $\dot{S}_{g,F}$ which is increased to 37.77% and 44.27% at Re is equal to 2756 and 21,820 against to water without insert.

Figure 8b notes down the $\dot{S}_{g,F}$ values of 0.05% nanofluid flow in a tube and with various coiled wire inserts

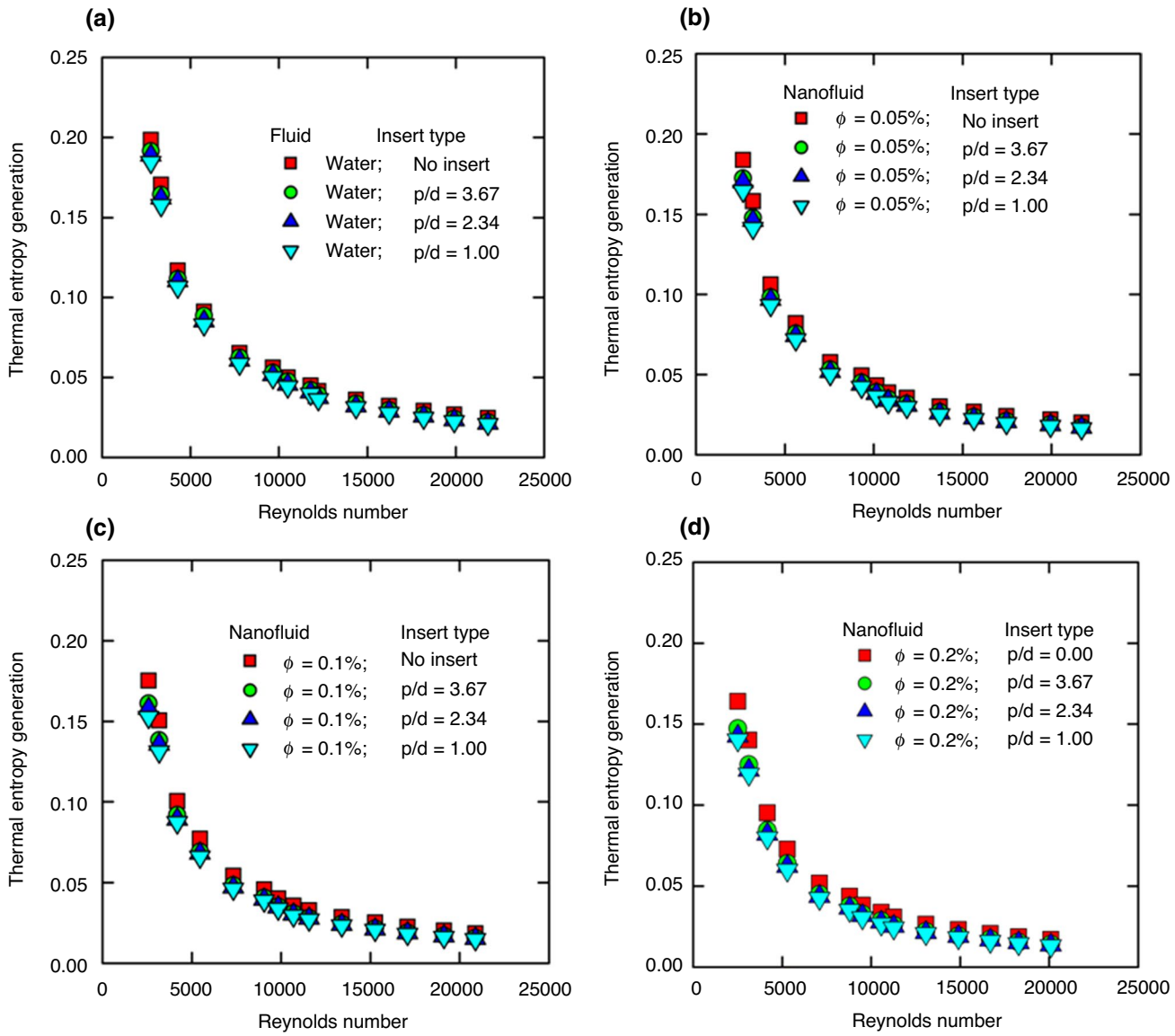

Fig. 7 Thermal entropy generation with effect of Reynolds numbers, volume concentrations and coiled wire inserts for **a** water, **b** $\phi = 0.05\%$, **c** $\phi = 0.1\%$ and **d** $\phi = 0.2\%$ nanofluids

under different Reynolds numbers. For $\phi = 0.05\%$ nanofluid with p/d of 3.67, the $\dot{S}_{g,F}$ which is decreased to 6.27% and 13.05% at Re is equal to 2649 and 21,678 against to $\phi = 0.05\%$ nanofluid without insert. However, for $\phi = 0.05\%$ nanofluid with p/d of 2.34, the $\dot{S}_{g,F}$ which is decreased to 7.47% and 15.84% at Re is equal to 2649 and 21,820 against to $\phi = 0.05\%$ nanofluid without insert. Moreover, for $\phi = 0.05\%$ nanofluid with p/d of 1.00, the $\dot{S}_{g,F}$ which is decreased to 10.53% and 18.27% at Re is equal to 2649 and 21,678 against to $\phi = 0.05\%$ nanofluid without insert.

Figure 8c represents the $\dot{S}_{g,F}$ values of $\phi = 0.1\%$ nanofluid flow in a tube and with various coiled wire inserts under different Reynolds numbers. For $\phi = 0.1\%$ nanofluid with p/d of 3.67, the $\dot{S}_{g,F}$ which is decreased to 8.03% and 15.24% at Re is equal to 2574 and 20,886 against to $\phi = 0.1\%$ nanofluid without insert. However, for $\phi = 0.1$ with p/d of 2.34, the $\dot{S}_{g,F}$ which is decreased to 9.90% and 18.02% at Re is equal to 2574 and 20,886 against to $\phi = 0.1\%$ $\dot{S}_{g,F}$ nanofluid without insert. Moreover, for $\phi = 0.1\%$ nanofluid with p/d of 1.00, the $\dot{S}_{g,F}$ which is decreased to 12.83% and 20.15% at Re is equal to 2574 and 20,886 against to $\phi = 0.1\%$ nanofluid without insert.

Figure 8d shows the $\dot{S}_{g,F}$ values of $\phi = 0.2\%$ nanofluid flow in a tube and with various coiled wire inserts under different Reynolds numbers. For $\phi = 0.2\%$ with p/d of 3.67, the $\dot{S}_{g,F}$ which is decreased to 10.20% and 17.47%

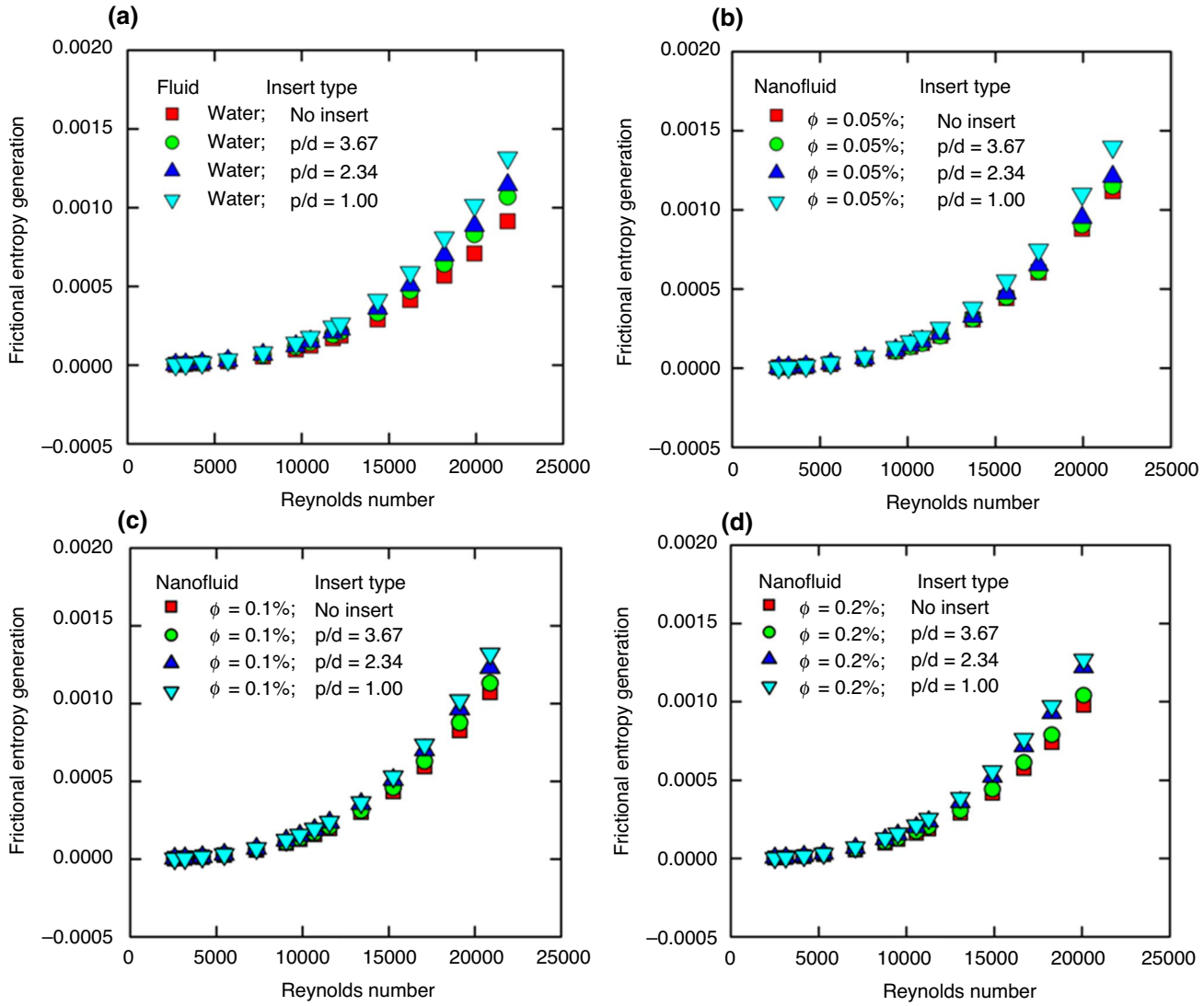

Fig. 8 Frictional entropy generation with effect of Reynolds numbers, volume concentrations and coiled wire inserts for **a** water, **b** $\phi = 0.05\%$, **c** $\phi = 0.1\%$ and **d** $\phi = 0.2\%$ nanofluids

at Re is equal to 2516 and 20,095 against to $\phi = 0.2\%$ nanofluid without insert. However, for $\phi = 0.2\%$ nanofluid with p/d of 2.34, the $\dot{S}_{g,F}$ which is decreased to 13.18% and 20.02% at Re is equal to 2516 and 20,095 against to $\phi = 0.2\%$ nanofluid without insert. Moreover, for $\phi = 0.2\%$ nanofluid with p/d of 1.00, the $\dot{S}_{g,F}$ which is decreased to 14.46% and 22.56% at Re is equal to 2516 and 20,095 against to $\phi = 0.2\%$ nanofluid without insert.

With the decrease in p/d value of coiled wire insert, the effective fluid turbulence takes place in the test tube resulting that decreased thermal entropy generation; this behavior was noticed for all the fluids.

Entropy generation number of hybrid nanofluids and with coiled wire inserts

Equation (10) evaluates the entropy generation number (N_s) of the system. The (N_s) for water and nanofluids in a tube and with various p/d values was analyzed. Figure 9a indicates the (N_s) of water flow with various p/d and at different Reynolds numbers. From the figure, the N_s value is decreased with an increase in Re and decrease in coiled wire p/d values. At the lower Re values, the N_s is high, whereas at higher Re values, the N_s is low. Hence, the higher values of N_s is presented here. The N_s for water in a plain tube and

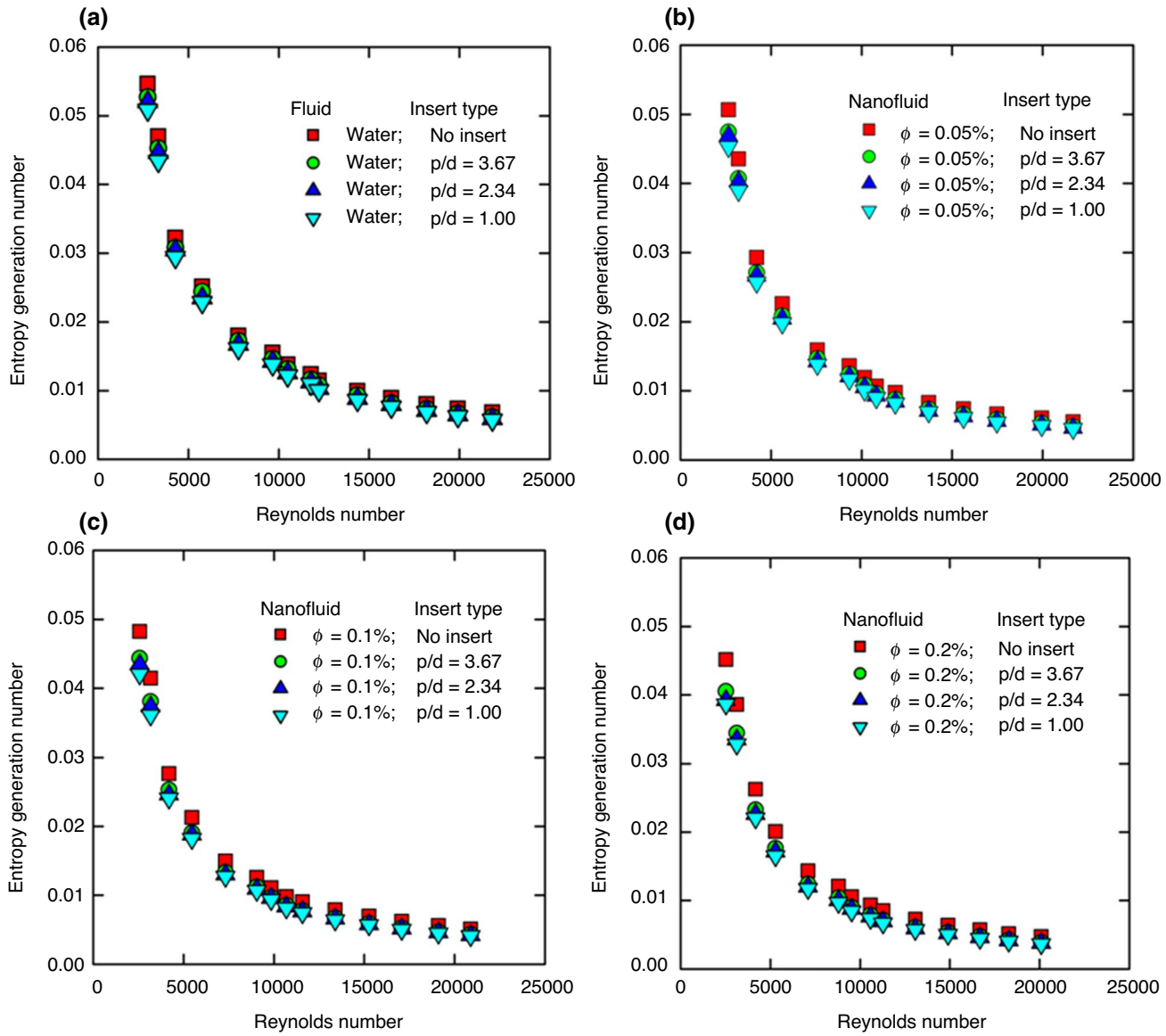

Fig. 9 Entropy generation number with effect of Reynolds numbers, volume concentrations and coiled wire inserts for **a** water, **b** $\phi = 0.05\%$, **c** $\phi = 0.1\%$ and **d** $\phi = 0.2\%$ nanofluids

with coiled wire insert of p/d = 3.67, 2.34 and 1.00 which is 0.0546, 0.0527, 0.0519 and 0.05, respectively, at *Re* is equal to 2756.

Figure 9b finds the N_s values of 0.05% vol. in a tube and with various coiled wire inserts under different Reynolds numbers. The similar fashion of decreased N_s value with an increased *Re* and decreased p/d of coiled wire inserts is observed. The N_s for 0.05% vol. in a plain tube and with coiled wire insert of p/d of 3.67, 2.34 and 1.00 which is 0.0506, 0.0474, 0.0468 and 0.045, respectively, at *Re* is equal to 2649.

Figure 9c identifies the N_s values of 0.1% vol. in a tube and with different p/d under different Reynolds numbers. The nature of decreased N_s value with an increased *Re* and decreased p/d of coiled wire inserts is observed. The N_s for $\phi = 0.1\%$ nanofluid flow in a plain tube and with coiled wire insert of p/d of 3.67, 2.34 and 1.00 which is 0.0482, 0.0443, 0.0434 and 0.042, respectively, at *Re* is equal to 2574.

Figure 9d indicates the N_s values of 0.2% vol. in a tube and with various with p/d values under different Reynolds numbers. The decreased N_s value with an increased *Re* and decreased p/d of coiled wire inserts was noticed. The N_s for 0.2% vol. in a plain tube and with coiled wire insert of p/d of 3.67, 2.34 and 1.00 which is 0.0451, 0.04057, 0.03922 and 0.0386, respectively, at *Re* is equal to 2516.

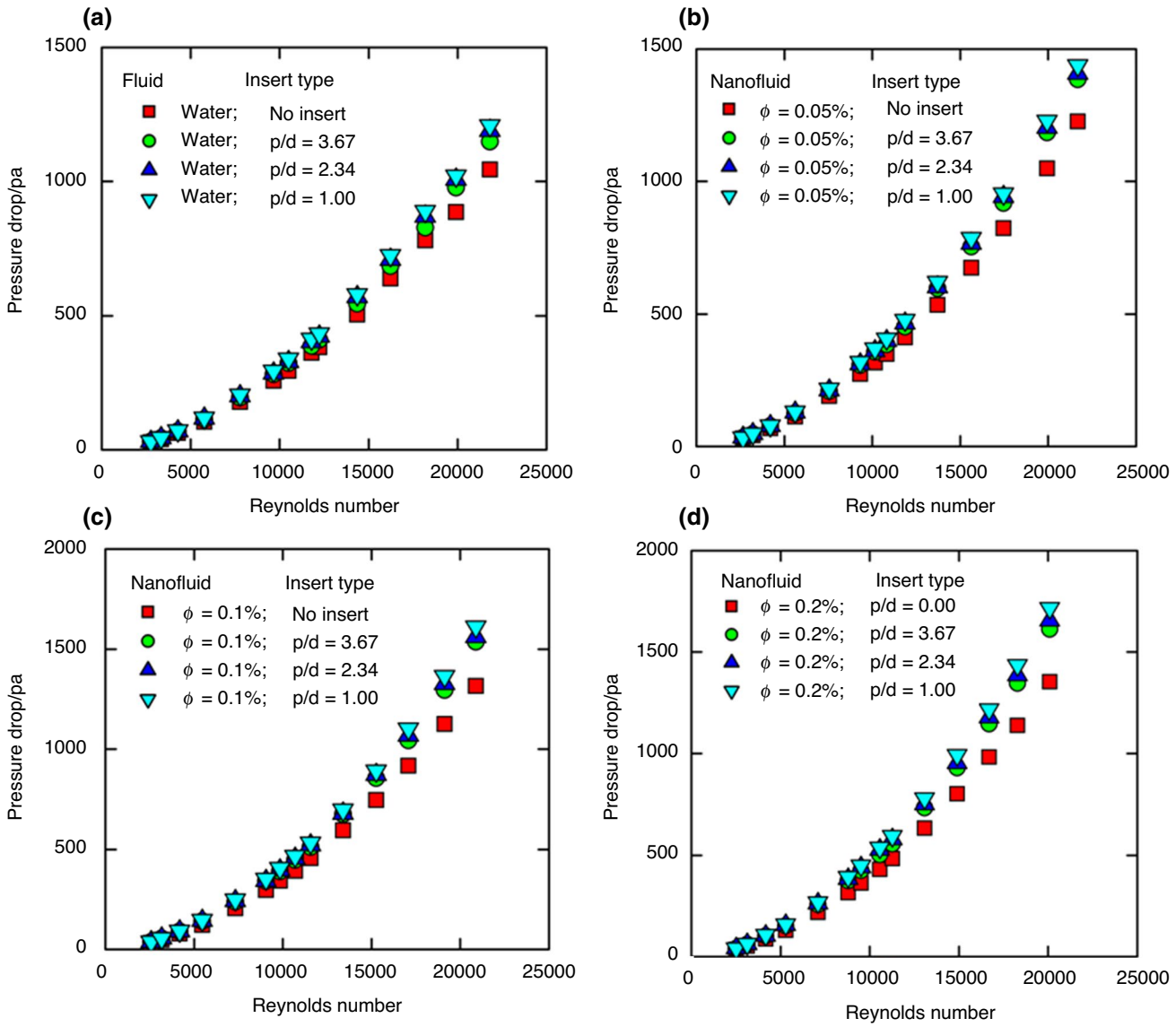

Fig. 10 Pressure drop with effect of Reynolds numbers, volume concentrations and coiled wire inserts for **a** water, **b** $\phi = 0.05\%$, **c** $\phi = 0.1\%$ and **d** $\phi = 0.2\%$ nanofluids

Pressure drop, friction factor and pumping power of hybrid nanofluids and with coiled wire inserts

Equation (12) evaluates the pressure drop (Δp) of the fluid. The Δp of various fluids and with coiled wire inserts is analyzed. Figure 10a indicates the Δp values of water flow in a tube and with various coiled wire inserts at different Reynolds numbers. Figure shows that the Δp is increased with an increase in Re and decrease in coiled wire p/d values. For water in a plain tube and with coiled wire insert of p/d of 3.67, the Δp which is increased to 6.90% and 10.04% at Re is equal to 2756 and 21,820 against water without insert. However, for the water in a plain tube and with coiled wire insert of p/d of 2.34, the Δp which is increased to 9.20% and 13.90% at Re is equal to 2756 and 21,820 against water without insert. Moreover, for the water in a plain tube and with coiled wire insert of p/d of 1.00, the Δp which is increased to 10.80% and 15.83% at Re is equal to 2756 and 21,820 against to water without insert.

Figure 10b indicates the Δp values of 0.05% vol. in a tube and with various coiled wire inserts under different Reynolds numbers. For 0.05% vol. in a plain tube and with coiled wire insert of p/d of 3.67, the Δp which is increased to 8.79% and 13% at Re is equal to 2649 and 21,678 against to 0.05% vol. without insert. However, for $\phi = 0.05\%$ nanofluid in a plain tube and with coiled wire insert of p/d of 2.34, the Δp which is increased to 10.78% and 14.80% at Re is equal to 2649 and 21,820 against to

0.05% vol. without insert. Moreover, for 0.05% vol. in a plain tube and with coiled wire insert of p/d of 1.00, the Δp which is increased to 12.99% and 17.32% at Re is equal to 2649 and 21,678 against to 0.05% vol. without insert.

Figure 10c presents the Δp values of $\phi = 0.1\%$ nanofluid flow in a tube and with various coiled wire inserts under different Reynolds numbers. For 0.1% vol. in a plain tube and with coiled wire insert of p/d of 3.67, the Δp which is increased to 11.96% and 16.79% at Re is equal to 2574 and 20,886 against to 0.1% vol. without insert. However, for 0.1% vol. in a plain tube and with coiled wire insert of p/d of 2.34, the Δp which is increased to 14.81% and 18.56% at Re is equal to 2574 and 20,886 against to $\phi = 0.1\%$ nanofluid without insert. Moreover, for 0.1% vol. in a plain tube and with coiled wire insert of p/d of 1.00, the Δp is increased to 17.87% and 22.47% at Re is equal to 2574 and 20,886 against to 0.1% vol. without insert.

Figure 10d notes the Δp values of 0.2% vol. in a tube and with various coiled wire inserts under different Reynolds numbers. For 0.2% vol. with p/d of 3.67, the Δp which is increased to 16.01% and 19.17% at Re is equal to 2516 and 20,095 against to 0.2% vol. without insert. However, for 0.2% vol. with p/d of 2.34, the Δp which is increased to 17.95% and 22.33% at Re is equal to 2516 and 20,095 against to 0.2% vol. without insert. Moreover, the 0.2% vol. with p/d of 1.00, the $\dot{S}_{g,H}$ which is increased to 20.96% and 26.90% at Re is equal to 2516 and 20,095 against to 0.2% vol. without insert. With the coiled wire inserts, the pressure drop is increased which is further increased for decrease in p/d value of coiled wire insert.

The obtained pressure drop is converted into non-dimensional friction factor from Eq. (13) for the case of water and nanofluids in a tube and with coiled wire inserts. The friction factor for water (Fig. 11a), 0.05% nanofluid (Fig. 11b), 0.1% nanofluid (Fig. 11c) and 0.2% nanofluid (Fig. 11d) at different concentrations, particle loadings and various p/d values were calculated and noticed that a maximum of 1.39-fold enhancement for 0.2% nanofluid with p/d of 1 was compared to water at a Reynolds number of 20,095. However, the used nanoparticle volume concentration in this study is very low concentrations, and hence, the prepared hybrid nanofluids will not increase the pump wear and also no corrosion was observed after the end of the experiments.

Figure 12 indicates the comparison of experimental friction factor of ND + Fe_3O_4 nanofluid with coiled wire inserts with Sundar et al. [58] of Fe_3O_4/water nanofluid. Decreasing p/d from 3.67 to 1.00, the friction factor is increased, and the similar nature has been observed by [58]. Sundar et al. [58] considered Fe_3O_4/water nanofluids with coiled wire inserts of 1.00, 1.34 and 1.79. The present data of ND + Fe_3O_4/water nanofluids with coiled wire inserts predict higher friction factor values compared to Sundar et al. [58] data. This is caused because of the use of hybrid nanofluids in the present study.

Equation (14) is used to estimate the pumping power of the nanofluid flow in a tube. With coiled wire inserts also, the pumping power is further estimated. The pumping power for water (Fig. 13a), 0.05% nanofluid (Fig. 13b), 0.1% nanofluid (Fig. 13c) and 0.2% nanofluid (Fig. 13d) at different concentrations, particle loadings and various p/d values were calculated and noticed that pumping power is increased with an increase in Re, ϕ and decrease in coiled wire inserts p/d values. At lower Reynolds number, the pumping power is lower and it is higher at higher Re values. For $\phi = 0.2\%$ and coiled wire inserts of p/d of 3.67, 2.34 and 1.00, the maximum of 0.459, 0.471 and 0.489 W was noticed at Re of 20,095, whereas for 0.2% nanofluid without inserts, it is 0.386 W. The pump power gain is there with the use of nanofluids, but compared to heat transfer enhancement, the pumping power enhancement is negligible.

Bejan Number

Equation (16) is used to calculate the Bejan number of hybrid nanofluid and with coiled wire inserts in a tube. When the Bejan number is reaching to 1, the influence of frictional exergy destruction of the system with influence of pressure drop is decreased. Large value of Bejan number shows the increase in entropy generation due to heat transfer in comparison with frictional entropy generation. Figure 14a–d indicates the Bejan number of water, 0.05%, 0.1% and 0.2% volume concentration of nanofluids and with coiled wire inserts. In all the figures, the Bejan number is nearly equal to 1 when the Reynolds number is lower, but with the gradual increase in Reynolds number, the Bejan number is decreased due to the increase in pressure drop and pumping power.

Exergy efficiency

Equation (8) estimates the exergy efficiency of water and hybrid nanofluids with and without coiled wire inserts. Figure 15a indicates the exergy efficiency of water flow in a tube and with various coiled wire inserts at different Reynolds numbers. From the figure, the exergy efficiency value is increased with an increase in Re and decrease in coiled wire p/d values. At the lower Re values, the exergy efficiency is lower, whereas at higher Re values, the exergy efficiency is higher. Hence, the higher exergy efficiency values are presented here. The exergy efficiency for water in a plain tube and with coiled wire insert of p/d of 3.67, 2.34 and 1.00 which is 18.95%, 28.61%, 31.65% and 37.88%, respectively, at Re is equal to 2756.

Figure 15b shows the exergy efficiency values of $\phi = 0.05\%$ nanofluid flow in a tube and with various coiled

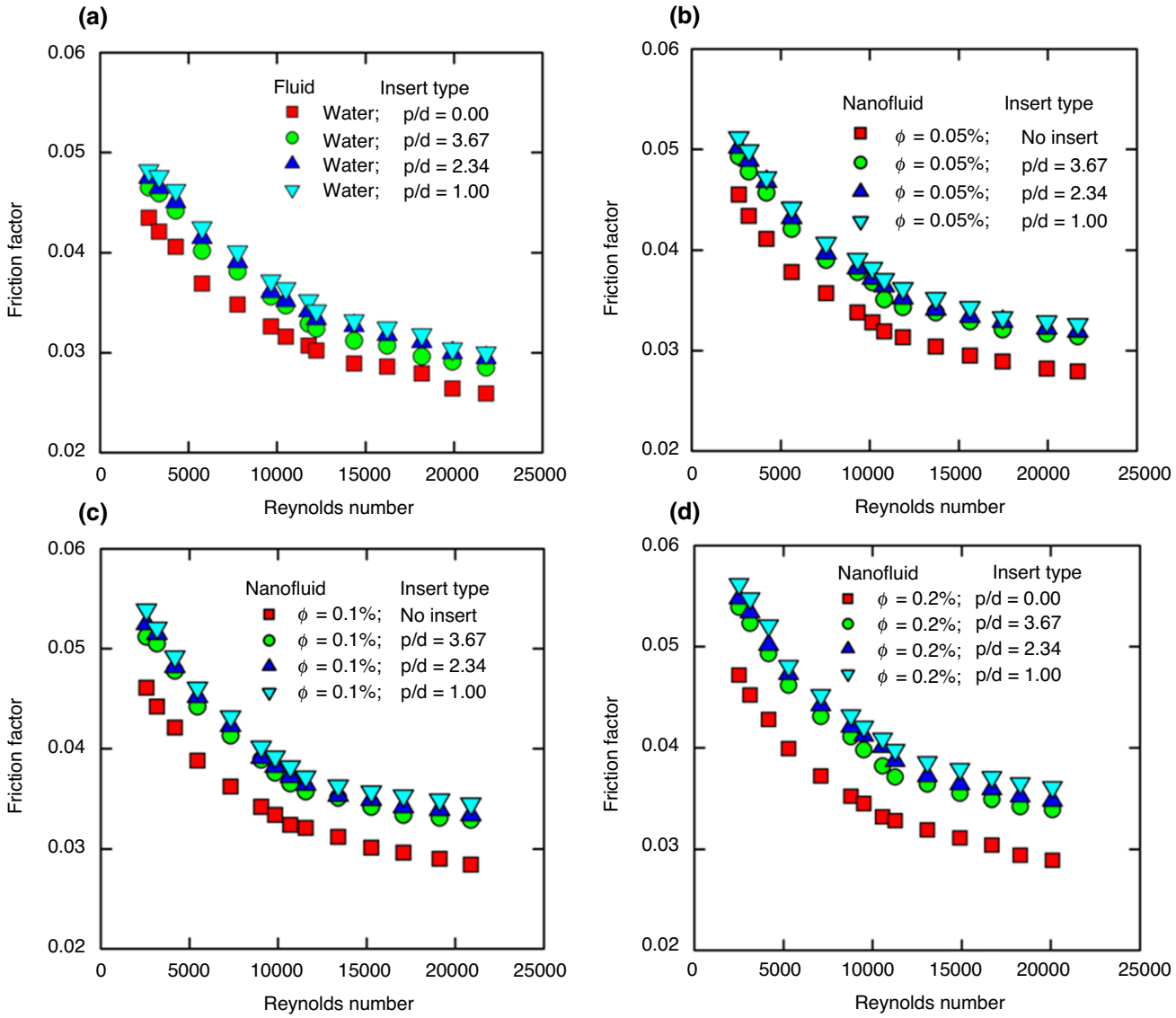

Fig. 11 Friction factor with effect of Reynolds numbers, volume concentrations and coiled wire inserts for **a** water, **b** $\phi = 0.05\%$, **c** $\phi = 0.1\%$ and **d** $\phi = 0.2\%$ nanofluids

wire inserts under different Reynolds numbers. The similar fashion of increased exergy efficiency with an increased *Re* and decreased p/d of coiled wire inserts was noticed. The exergy efficiency for $\phi = 0.05\%$ nanofluid flow in a plain tube and with coiled wire insert of p/d of 3.67, 2.34 and 1.00 which is 21.73%, 34.33%, 37.53% and 44.64%, respectively, at *Re* is equal to 2649.

Figure 15c indicates the exergy efficiency of $\phi = 0.1\%$ nanofluid flow in a tube and with various coiled wire inserts at different Reynolds numbers. The nature of increased exergy efficiency value with an increased *Re* and decreased p/d of coiled wire inserts was noticed. The exergy efficiency for the Poisson structure on = 0.1% nanofluid flow in a plain tube and with coiled wire insert of p/d = 3.67, 2.34 and 1.00 which is 22.62%, 37.42%, 40.76% and 47.89%, respectively, at *Re* is equal to 2574. Figure 15d predicts the exergy efficiency of $\phi = 0.2\%$ nanofluid flow in a tube and with various coiled wire inserts under different Reynolds numbers. The exergy efficiency for $\phi = 0.2\%$ nanofluid flow in a plain tube and with coiled wire insert of p/d of 3.67, 2.34 and 1.00 which is 24.06%, 40.85%, 44.22% and 51.58%, respectively, at *Re* is equal to 2516.

Proposed correlations

Nusselt number

Sundar et al. [58] and Hamid et al. [41] developed Nusselt number correlation for Fe_3O_4/water nanofluid with coiled

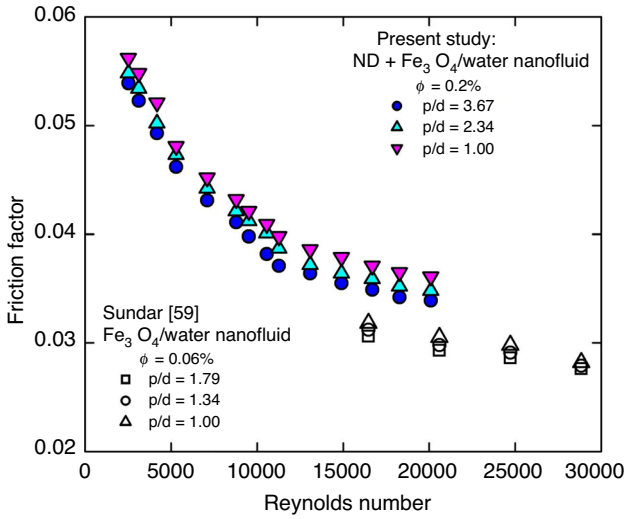

Fig. 12 Comparison of experimental friction factor of ND + Fe_3O_4 nanofluid with coiled wire inserts with Sundar et al. [58] of Fe_3O_4/water nanofluid

wire inserts and TiO_2-SiO_2/60:40% EG/W nanofluid with coiled wire inserts. Their correlations are presented below:

Sundar et al. [58],

$$Nu = 0.0565 Re^{0.8} \mathrm{Pr}^{0.4} (1+\phi)^{2.051} \left(1+\frac{p}{d}\right)^{0.06}$$
$$16000 < Re < 30000; 5.42 < \mathrm{Pr} < 6.68$$
$$0 < \phi < 0.06\%; 0 < p/d < 1.79 \quad (20)$$

Hamid et al. [41],

$$Nu = 1.65 \times 10^{4} Re^{0.705} \mathrm{Pr}^{2.64} \left(1+\frac{\phi}{100}\right)^{8.58} \left(\frac{p}{d}\right)^{-0.411}$$
$$2000 < Re < 11000;$$
$$0 < \phi < 3.0\%; 0.83 < p/d < 4.17 \quad (21)$$

From the experimental data, Nusselt number correlation which is developed in similar lines of Sundar et al. [58] and Hamid et al. [41] by considering non-dimensional parameters of Reynolds number, Prandtl number, Nusselt number, particle volume concentration and pitch/diameter ratio is used to develop the correlation.

$$Nu = 0.1108 \times 10^{-4} Re^{1.303} \mathrm{Pr}^{2.048} (1+\phi)^{0.7192} \left(1+\frac{p}{d}\right)^{0.04892}$$
$$2516 < Re < 21820; 5.65 < \mathrm{Pr} < 7.79$$
$$0 < \phi < 0.2\%; 0 < p/d < 3.67 \quad (22)$$

The experimental Nusselt number is compared with Eq. (22) data in Fig. 16.

Friction factor

Sundar et al. [58] and Hamid et al. [41] developed friction factor correlation for Fe_3O_4/water nanofluid with coiled wire inserts and TiO_2–SiO_2/60:40% EG/W nanofluid with coiled wire inserts. Their correlations are presented below:

Sundar et al. [58],

$$f = 0.2891 Re^{-0.24} (1+\phi)^{1.535} \left(1+\frac{p}{d}\right)^{0.04143}$$
$$16000 < Re < 30000;$$
$$0 < \phi < 0.06\%; 0 < p/d < 1.79 \quad (23)$$

Hamid et al. [41],

$$f = 4.16 Re^{-0.269} \left(1+\frac{\phi}{100}\right)^{3.31} \left(1+\frac{p}{d}\right)^{-1.17}$$
$$2000 < Re < 11000;$$
$$0 < \phi < 3.0\%; 0 < p/d < 4.17 \quad (24)$$

From the experimental data, friction factor correlation which is developed in similar lines of Sundar et al. [58] and Hamid et al. [41] by considering non-dimensional parameters of Reynolds number, friction factor, particle volume concentration and pitch/diameter ratio is used to develop the correlation.

$$f = 0.2969 Re^{-0.2388} (1+\phi)^{0.5874} \left(1+\frac{p}{d}\right)^{0.07188}$$
$$2516 < Re < 21820;$$
$$0 < \phi < 0.2\%; 0 < p/d < 3.67 \quad (25)$$

The experimental friction factor is compared with Eq. (25) data in Fig. 17.

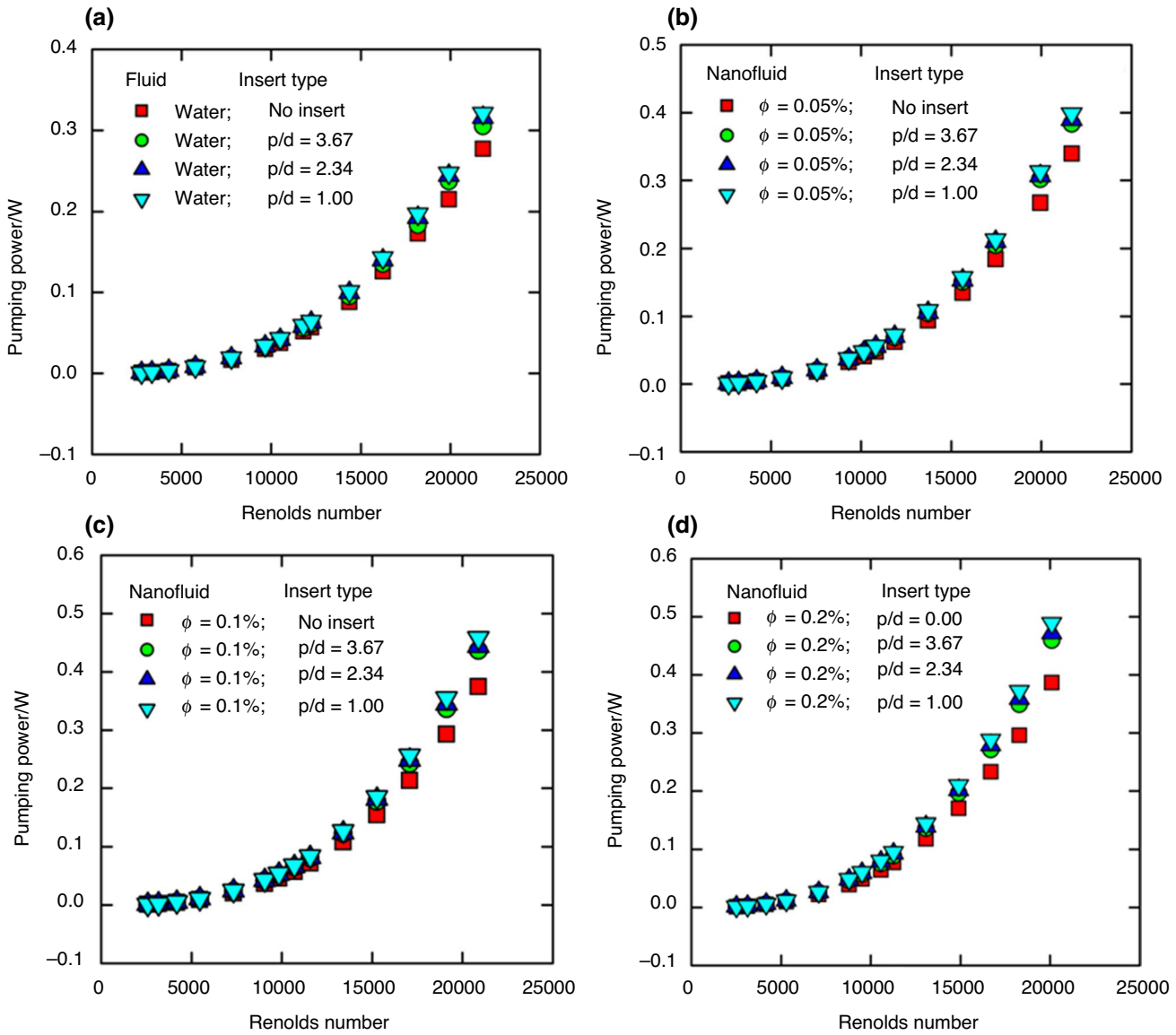

Fig. 13 Pumping power with effect of Reynolds numbers, volume concentrations and coiled wire inserts for **a** water, **b** $\phi = 0.05\%$, **c** $\phi = 0.1\%$ and **d** $\phi = 0.2\%$ nanofluids

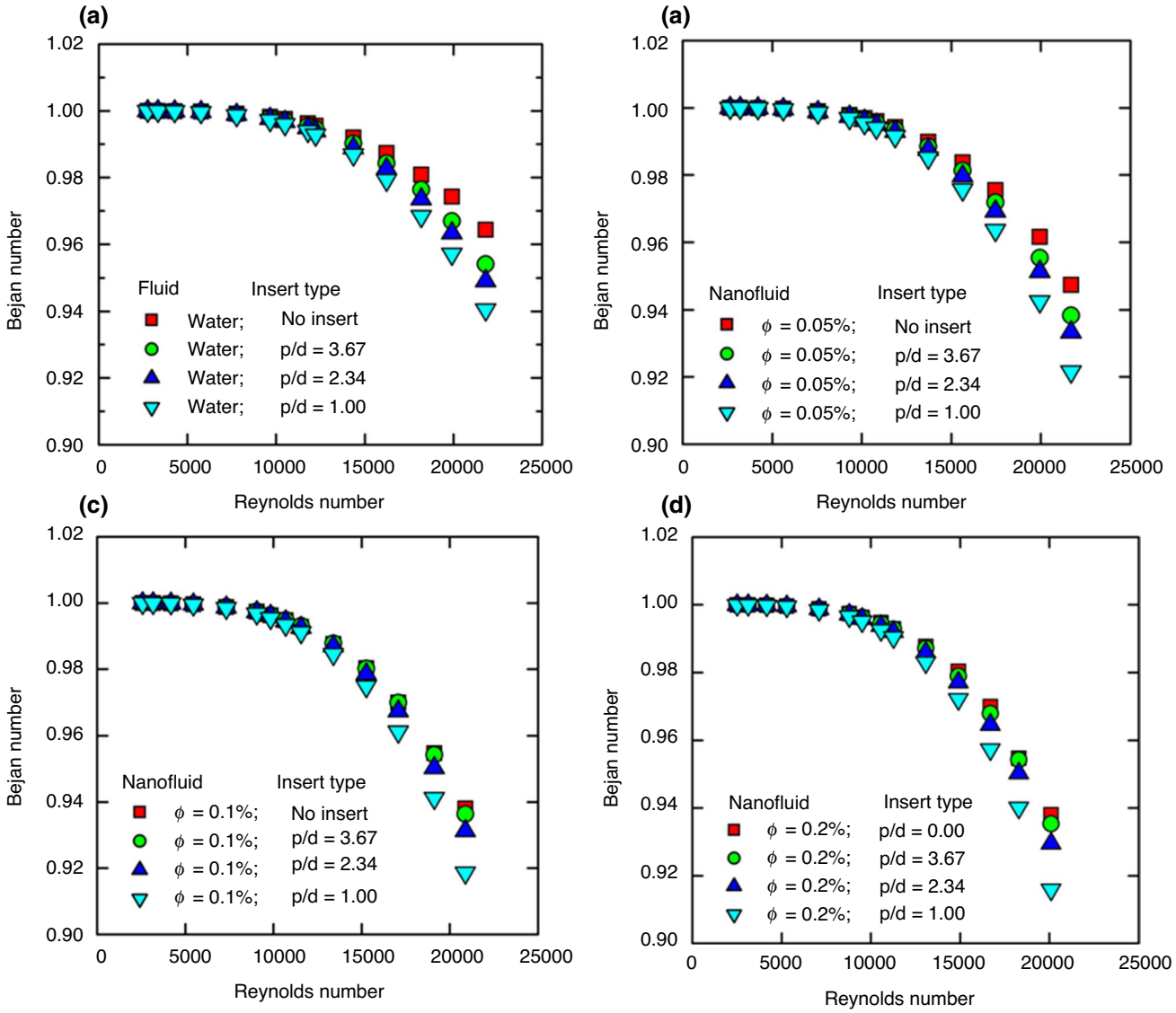

Fig. 14 Bejan number with effect of Reynolds numbers, volume concentrations and coiled wire inserts for **a** water, **b** $\phi = 0.05\%$, **c** $\phi = 0.1\%$ and **d** $\phi = 0.2\%$ nanofluid

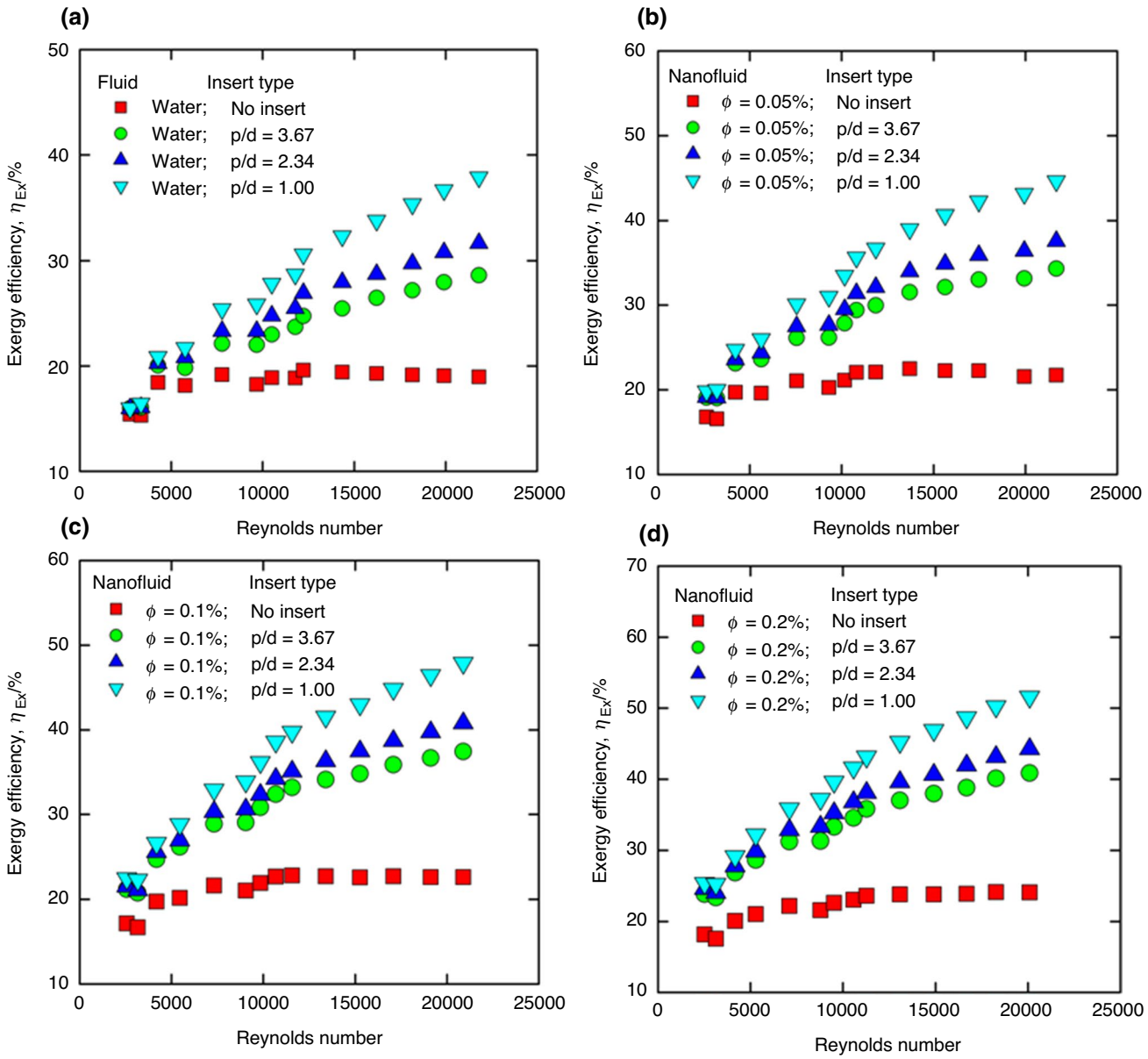

Fig. 15 Exergy efficiency with effect of Reynolds numbers, volume concentrations and coiled wire inserts for **a** water, **b** ϕ=0.05%, **c** ϕ=0.1% and **d** ϕ=0.2% nanofluid

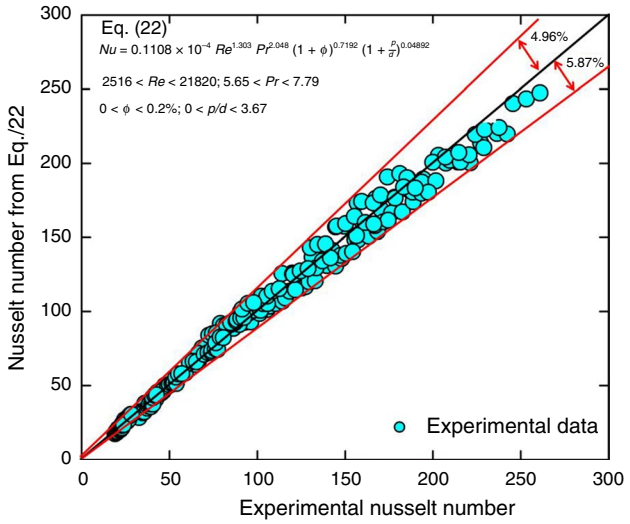

Fig. 16 Comparison between experimental Nusselt number and Eq. (22) data

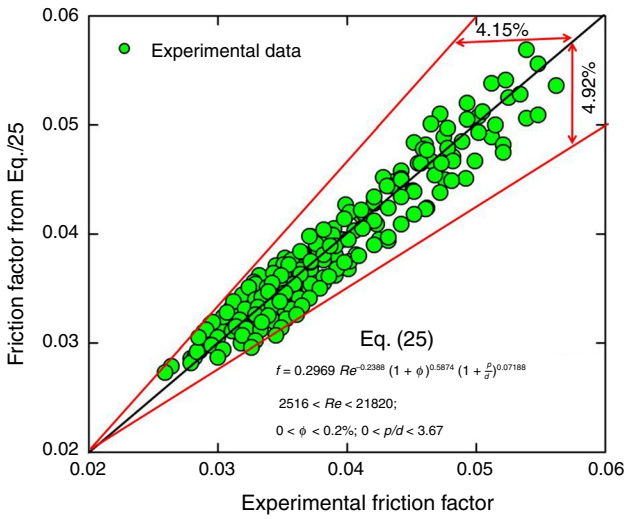

Fig. 17 Comparison between experimental friction factor and Eq. (25) data

Conclusions

Experiments were conducted to analyze the heat transfer coefficient, Nusselt number, friction factor, pumping power, thermal and frictional entropy generation of ND + Fe_3O_4/water hybrid nanofluid flow in a tube and with coiled wire inserts under turbulent flow conditions. When the particle loadings are increased from 0.05% to 0.2%, the heat transfer coefficient, Nusselt number, pressure drop and friction factor are increased and it is further increased by inserting coiled wire inserts inside the nanofluid flow. By using 0.2% vol. of hybrid nanofluid and at *Re* of 20,095 in a tube, the heat transfer coefficient and Nusselt number are increased to 44.36% and 29.55%; and those are further increased to 107.19% and 66.36% by inserting coiled wire insert of p/d = 1 compared to base fluid data.

Moreover, for 0.2% vol. of hybrid nanofluid in a tube, the friction factor, pressure drop and pumping power are raised to 11.1%, 29.58% and 39.49%; and those are further enhanced to 38.84%, 64.44% and 76.53% by inserting coiled wire insert of p/d = 1 compared to water data at *Re* of 20,095. The thermal entropy generation is decreased to 30.80% and it is further decreased to 46.34% by using coiled wire insert of p/d = 1 at 0.2% vol. and at *Re* of 20,095 compared to water. When using the water in a tube, the exergy efficiency is 18.95% and it is increased to 24.06% by using 0.2% vol. of nanofluid and it is further increased to 51.58% by using 0.2% vol. of nanofluid and with coiled wire insert of p/d = 1 at *Re* of 20,095.

Finally, the study provides information of hybrid nanofluids and with coiled wire inserts is the promising opinion for better heat transfer and exergy efficiency of the tube. Similarly, thermal entropy generation is further decreased by using the coiled wire inserts. In the other side, the friction factor, pressure drop and pumping power are slightly increased.

Appendix A: uncertainty analysis

The procedure of Kline and McClintock [61] is used for error analysis. The errors are based on the least counts and the sensitivities of the measuring instruments used in the present study, and those are shown in Table 6. The equations for Reynolds number, Nusselt number, friction factor, entropy generation and exergy efficiency are given below. The calculated uncertainty values are indicated in Table 7.

Reynolds number,

$$Re = \frac{4 \cdot \dot{m}}{\pi \cdot D \cdot \mu} \tag{A1}$$

$$\frac{\Delta Re}{Re} = \left[\left(\frac{\Delta \dot{m}}{\dot{m}}\right)^2 + \left(\frac{\Delta d}{d}\right)^2\right]^{0.5} \tag{A2}$$

$$\frac{\Delta Re}{Re} = \left[\left(\frac{7.01 \times 10^{-4}}{0.2647}\right)^2 + \left(\frac{0.0002}{0.019}\right)^2\right]^{0.5} \tag{A3}$$

$$\frac{\Delta Re}{Re} = 0.0108 = 1.08\% \tag{A4}$$

Heat flux,

$$q = \frac{Q}{A} \Rightarrow \frac{V \times I}{\pi DL} \tag{A5}$$

$$\frac{\Delta q}{q} = \left[\left(\frac{\Delta V}{V}\right)^2 + \left(\frac{\Delta I}{I}\right)^2\right]^{0.5} \tag{A6}$$

$$\frac{\Delta q}{q} = \left[\left(\frac{0.1}{220}\right)^2 + \left(\frac{1}{20}\right)^2\right]^{0.5} \tag{A7}$$

$$\frac{\Delta q}{q} = 0.0500 = 5.00\% \tag{A8}$$

Heat transfer coefficient,

$$h = \frac{q}{(T_s - T_m)} \tag{A9}$$

$$\frac{\Delta h}{h} = \left[\left(\frac{\Delta q}{q}\right)^2 + \left(\frac{\Delta T_s}{T_s}\right)^2 + \left(\frac{\Delta T_m}{T_m}\right)^2\right]^{0.5} \tag{A10}$$

$$\frac{\Delta h}{h} = \left[(0.05)^2 + \left(\frac{0.1}{50.92}\right)^2 + \left(\frac{0.1}{35.67}\right)^2\right]^{0.5} \tag{A11}$$

Table 6 Uncertainty analysis

S. No	Quantity	Maximum value	Probable error
1	D	0.019 m	0.0002 m
2	$\dot{m}$	0.2647 kg	7.01×10^{-4}
3	V	220	0.1 °C
4	I	20	1
5	T_s	50.92 °C	0.1 °C
6	T_b	35.67 °C	0.1 °C
7	T_a	30 °C	0.1 °C
8	T_{in}	30 °C	0.1 °C
9	T_{out}	40.51 °C	0.1 °C
10	Δp	1600 Pa	0.1 Pa

Table 7 Uncertainty values

S. No	Parameter	Uncertainty
1	Reynolds number, *Re*	1.08%
2	Heat flux,*q*	5.00%
3	Heat transfer coefficient, h	5.011%
4	Nusselt number, Nu	5.011%
5	Friction factor, f	2.16%
6	Thermal entropy generation	11.93%
7	Exergy efficiency	12.94%

$$\frac{\Delta h}{h} = 0.05011 = 5.011\% \tag{A12}$$

Nusselt number,

$$Nu = \frac{hD}{k} \tag{A13}$$

$$\frac{\Delta Nu}{Nu} = \left[\left(\frac{\Delta h}{h}\right)^2\right]^{0.5} \tag{A14}$$

$$\frac{\Delta Nu}{Nu} = 0.05011 = 5.011\% \tag{A15}$$

Pressure drop

$$\frac{\Delta(\Delta p)}{\Delta p} = \frac{0.1}{1600} = 0.0000625 \tag{A16}$$

Friction factor,

$$f = \frac{\Delta P}{\left(\frac{L}{D}\right)\left(\frac{\rho v^2}{2}\right)} \tag{A17}$$

The velocity v in Eq. (A17) is expressed in terms of Reynolds number, and then, it becomes Eq. (A18).

$$v = \frac{Re \cdot \pi \cdot D \cdot \mu}{4 \cdot \rho \cdot A}, \text{ then } v^2 = \left(\frac{Re \cdot \pi \cdot D \cdot \mu}{4 \cdot \rho \cdot A}\right)^2 \tag{A18}$$

The terms $\pi, D, \mu, \rho, A and L$ are numbers only, and then, v depends on Reynolds number. Rewrite Eq. (A17) into Eq. (A19).

$$\frac{\Delta f}{f} = \left[\left(\frac{\Delta(\Delta P)}{\Delta P}\right)^2 + \left(\frac{\Delta Re}{Re}\right)^2\right]^{0.5} \tag{A19}$$

$$\frac{\Delta f}{f} = \left[\left(\frac{\Delta(\Delta P)}{\Delta P}\right)^2 + \left(2\frac{\Delta Re}{Re}\right)^2\right]^{0.5} \tag{A20}$$

$$\frac{\Delta f}{f} = \left[(0.0000625)^2 + (2 \times 0.0108)^2\right]^{0.5} \tag{A21}$$

$$\frac{\Delta f}{f} = 0.0216 = 2.16\% \tag{A22}$$

Thermal entropy generation,

$$\dot{S}_{g,H} = \frac{Q_{ag}^2}{Nu \cdot \pi \cdot k \cdot T_{in} \cdot T_{out} \cdot L} \tag{A23}$$

$$\frac{\Delta \dot{S}_{g,H}}{\dot{S}_{g,H}} = \left[\left(2\frac{\Delta Q_{av}}{Q_{av}}\right)^2 + \left(\frac{\Delta Nu}{Nu}\right)^2 + \left(\frac{\Delta T_{in}}{T_{in}}\right)^2 + \left(\frac{\Delta T_{out}}{T_{out}}\right)^2\right]^{0.5} \quad \text{(A24)}$$

$$\frac{\Delta \dot{S}_{g,H}}{\dot{S}_{g,H}} = \left[(2\times 0.0500)^2 + (0.05011)^2 + \left(\frac{0.1}{30}\right)^2 + \left(\frac{0.1}{40.51}\right)^2\right]^{0.5} \quad \text{(A25)}$$

$$\frac{\Delta \dot{S}_{g,H}}{\dot{S}_{g,H}} = 0.1193 = 11.93\% \quad \text{(A26)}$$

Exergy efficiency,

$$\eta_{ex} = 1 - \frac{T_a \cdot \dot{S}_{g,H}}{\left[1 - \left(\frac{T_a}{T_s}\right)\right] Q_{ag}} \quad \text{(A27)}$$

$$\frac{\Delta \eta_{ex}}{\eta_{ex}} = \left[\left(\frac{\Delta \dot{S}_{g,H}}{\dot{S}_{g,H}}\right)^2 + \left(\frac{\Delta T_a}{T_a}\right)^2 + \left(\frac{\Delta T_s}{T_s}\right)^2 + \left(\frac{\Delta Q_{ag}}{Q_{ag}}\right)^2\right]^{0.5} \quad \text{(A28)}$$

$$\frac{\Delta \eta_{ex}}{\eta_{ex}} = \left[(0.1193)^2 + \left(\frac{0.1}{30}\right)^2 + \left(\frac{0.1}{50.92}\right)^2 + (0.050)^2\right]^{0.5} \quad \text{(A29)}$$

$$\frac{\Delta \eta_{ex}}{\eta_{ex}} = 0.1294 = 12.94\% \quad \text{(A30)}$$

Acknowledgements The authors, LSS (Ref. 045-88-ARH/2018 and CEEC 2018 individual call) and EVR (Ref. 032-88-ARH/2018), acknowledge the Fundaç˜ao para a Ciencia e a Tecnologia, Portugal, for their projects; LSS and ACMS also acknowledge FCT grant UID/EMS/ 00481/2013-FCT and the infrastructures support CENTRO-01-0145-FEDER-022083.

References

1. Choi SUS. Enhancing thermal conductivity of fluids with nanoparticles. ASME International Mechanical Engineering Congress and Exposition. San Francisco, CA (1995)
2. Esfe MH, Motallebi SM, Bahiraei M. Employing response surface methodology and neural network to accurately model thermal conductivity of TiO_2–water nanofluid using experimental data. Chin J Phys. 2021;70:14–25.
3. Riahi A, Khamlich S, Balghouthi M, Khamliche T, Doyle TB, Dimassi W, Guizani A, Maaza M. Study of thermal conductivity of synthesized Al_2O_3-water nanofluid by pulsed laser ablation in liquid. J Mol Liquids. 2020;304:112694.
4. Li Z, Asadi S, Karimipour A, Abdollahi A, Tlili I. Experimental study of temperature and mass fraction effects on thermal conductivity and dynamic viscosity of SiO_2-oleic acid/liquid paraffin nanofluid. Int Commun Heat Mass Transf. 2020;110:104436.
5. Sundar LS, Singh MK, Sousa ACM. Investigation of thermal conductivity and viscosity of Fe_3O_4 nanofluid for heat transfer applications. Int Commun Heat Mass Transf. 2013;44:7–14.
6. Liu MS, Lin MCC, Huang IT, Wang CC. Enhancement of thermal conductivity with CuO for nanofluids. Chem Eng Technol. 2006;29:72–7.
7. Guo W, Li G, Zheng Y, Dong C. Measurement of the thermal conductivity of SiO_2 nanofluids with an optimized transient hot wire method. Thermochim Acta. 2018;661:84–97.
8. Sundar LS, Singh MK, Bidkin I, Sousa ACM. Experimental investigations in heat transfer and friction factor of magnetic Ni nanofluid flowing in a tube. Int J Heat Mass Transf. 2014;70:224–34.
9. Ali HM. In tube convection heat transfer enhancement: SiO_2 aqua based nanofluids. J Mol Liquids. 2020;308:113031.
10. Kim S, Tserengombo B, Choi SH, Noh J, Huh S, Choi B, Chung H, Kim J, Jeong H. Experimental investigation of heat transfer coefficient with Al_2O_3 nanofluid in small diameter tubes. Appl Therm Eng. 2019;146:346–55.
11. Azeez K, Hameed AF, Hussein AM. Nanofluid heat transfer augmentation in a double pipe heat exchanger. AIP Conf Proc. 2020;2213: 020059. https://doi.org/10.1063/5.0000243.
12. Azmi WH, Sharma KV, Sarma PK, Mamat R, Najafi G. Heat transfer and friction factor of water based TiO_2 and SiO_2 nanofluids under turbulent flow in a tube. Int Commun Heat Mass Transf. 2014;59:30–8.
13. Duangthongsuk W, Wongwises S. Heat transfer enhancement and pressure drop characteristics of TiO_2–water nanofluid in a double-tube counter flow heat exchanger. Int J Heat Mass Transfer. 2009;52:2059–67.
14. Albadr J, Tayal S, Alasadi M. Heat transfer through heat exchanger using Al_2O_3 nanofluid at different concentrations. Case Stud Thermal Eng. 2013;1:38–44.
15. Godson L, Deepak K, Enoch C, Jefferson B, Raja B. Heat transfer characteristics of silver/water nanofluids in a shell and tube heat exchanger. Arch Civil Mech Eng. 2014;14:489–96.
16. Liu MS, Lin MCC, Huang IT, Wang CC. Enhancement of thermal conductivity with carbon nanotube for nanofluids. Int Commun Heat Mass Transf. 2005;32:1202–10.
17. Sundar LS, Hashim Farooky M, Naga Sarada S, Singh MK. Experimental thermal conductivity of ethylene glycol and water mixture based low volume concentration of Al_2O_3 and CuO nanofluids. Int Commun Heat Mass Transf. 2013;41:41–6.
18. Sundar LS, Singh MK, Ramana EV, Singh BK, Gracio J, Sousa ACM. Enhanced thermal conductivity and viscosity of nanodiamond-nickel nanocomposite nanofluids. Sci Rep. 2014;4:4039.
19. Nine MJ, Batmunkh M, Kim JH, Chung HS, Jeong HM. Investigation of Al_2O_3-MWCNTs hybrid dispersion in water and their thermal characterization. J Nanosci Nanotechnol. 2012;12:4553–9.
20. Sundar LS, Singh MK, Ferro MC, Sousa ACM. Experimental investigation of the thermal transport properties of graphene oxide/Co_3O_4 hybrid nanofluids. Int Commun Heat Mass Transf. 2017;84:1–10.
21. Sundar LS, Irurueta GO, Ramana EV, Singh MK, Sousa ACM. Thermal conductivity and viscosity of hybrid nanofluids prepared with magnetic nanodiamond-cobalt oxide (ND-Co_3O_4) nanocomposite. Case Stud Therm Eng. 2016;7:66–77.
22. Fazeli I, Emami MRS, Rashidi A. Investigation and optimization of the behavior of heat transfer and flow of MWCNT-CuO hybrid nanofluid in a brazed plate heat exchanger using response surface methodology. Int Commun Heat Mass Transf. 2021;122:105175.
23. Zhang S, Lu L, Wen T, Dong C. Turbulent heat transfer and flow analysis of hybrid Al_2O_3-CuO/water nanofluid: An experiment and CFD simulation study. Appl Therm Eng. 2021;188:116589.
24. Chawhan SS, Barai DP, Bhanvase BA. Investigation on thermophysical properties, convective heat transfer and performance evaluation of ultrasonically synthesized Ag-doped TiO_2 hybrid nanoparticles based highly stable nanofluid in a minichannel.

Therm Sci Eng Prog. 2021. https://doi.org/10.1016/j.tsep.2021.100928.
25. Li X, Wang H, Luo B. The thermophysical properties and enhanced heat transfer performance of SiC-MWCNTs hybrid nanofluids for car radiator system. Col Surf A Physicochem Eng Aspects. 2021;612:125968.
26. Abbas F, Ali HM, Shaban M, Janjua MM, Shah TR, Doranehgard MH, Ahmadlouydarab M, Farukh F. Towards convective heat transfer optimization in aluminum tube automotive radiators: Potential assessment of novel Fe_2O_3-TiO_2/water hybrid nanofluid. J Taiwan Inst Chem Eng. 2021;124:424–36.
27. Krishna VM, Kumar MS, Mahesh O, Kumar PS. Numerical investigation of heat transfer and pressure drop for cooling of microchannel heat sink using MWCNT-CuO-Water hybrid nanofluid with different mixture ratio. Mater Today Proc. 2021;42:969–74.
28. Iftikhar N, Rehman A, Sadaf H. Theoretical investigation for convective heat transfer on Cu/water nanofluid and (SiO_2-copper)/water hybrid nanofluid with MHD and nanoparticle shape effects comprising relaxation and contraction phenomenon. Int Commun Heat Mass Transf. 2021;120:105012.
29. Sundar LS, Singh MK, Sousa ACM. Turbulent heat transfer and friction factor of nanodiamond-nickel hybrid nanofluids flow in a tube: an experimental study. Int J Heat Mass Transf. 2018;117:223–34.
30. Sundar LS, Singh MK, Sousa ACM. Enhanced heat transfer and friction factor of MWCNT–Fe_3O_4/water hybrid nanofluid. Int Commun Heat Mass Transf. 2014;52:73–83.
31. Gupta M, Singh V, Said Z. Heat transfer analysis using zinc ferrite/water (Hybrid) nanofluids in a circular tube: An experimental investigation and development of new correlations for thermophysical and heat transfer properties. Sustain Energy Technol Assess. 2020;39:100720.
32. Saleh B, Sundar LS. Experimental study on heat transfer, friction factor, entropy and exergy efficiency analyses of a corrugated plate heat exchanger using Ni/water nanofluids. Int J Thermal Sci. 2021;165:106935.
33. Saleh B, Sundar LS. Entropy generation and exergy efficiency analysis of ethylene glycol-water based nanodiamond + Fe_3O_4 hybrid nanofluids in a circular tube. Powder Technol. 2021;380:430–42.
34. Kumar V, Tiwari AK, Ghosh SK. Exergy analysis of hybrid nanofluids with optimum concentration in a plate heat exchanger. Mater Res Exp. 2018;5:065022.
35. Dezfulizadeh A, Aghaei A, Joshaghani AH, Najafizadeh MM. Exergy efficiency of a novel heat exchanger under MHD effects filled with water-based Cu–SiO_2-MWCNT ternary hybrid nanofluid based on empirical data. J Thermal Anal Calorim. 2021. https://doi.org/10.1007/s10973-021-10867-3.
36. Sundar LS, Ramana EV, Said Z, Pereira AMB, Sousa ACM. Heat transfer of rGO/CO_3O_4 hybrid nanomaterial-based nanofluids and twisted tape configurations in a tube. J Therm Sci Eng Appl. 2021;13(031004):1–15.
37. Sundar LS, Otero-Irurueta G, Singh MK, Sousa ACM. Heat transfer and friction factor of multi-walled carbon nanotubes–Fe_3O_4 nanocomposite nanofluids flow in a tube with/without longitudinal strip inserts. Int J Heat Mass Transf. 2016;100:691–703.
38. Reddy MCS, Vasudeva RV. Experimental investigation of heat transfer coefficient and friction factor of ethylene glycol water based TiO_2 nanofluid in double pipe heat exchanger with and without helical coil inserts. Int Commun Heat Mass Transf. 2014;50:68–76.
39. Sundar LS, Mathew B, Sefelnasr A, Sherif M, Sharma KV. Enhanced heat transfer and thermal performance factor of coiled wire inserted rGO/Co_3O_4 hybrid nanofluid circulating in a horizontal tube. J Enhanced Heat Transf. 2021;28:77–103.
40. Sundar LS, Said Z, Saleh B, Singh MK, Sousa ACM. Combination of Co_3O_4 deposited rGO hybrid nanofluids and longitudinal strip inserts: thermal properties, heat transfer, friction factor, and thermal performance evaluations. Therm Sci Eng Prog. 2020;20:100695.
41. Hamid KA, Azmi WH, Mamat R, Sharma KV. Heat transfer performance of TiO_2–SiO_2 nanofluids in a tube with wire coil inserts. Appl Therm Eng. 2019;152:275–86.
42. Azmi WH, Hamid KA, Ramadhan AI, Shaiful AIM. Case Stud Therm Eng. 2021;25:100899.
43. Singh SK, Sarkar J. Improving hydrothermal performance of hybrid nanofluid in double tube heat exchanger using tapered wire coil turbulator. Adv Powder Technol. 2020;31:2092–100.
44. Shahsavar A, Bakhshizadeh MA, Arici M, Afrand M, Rostami S. Numerical study of the possibility of improving the hydrothermal performance of an elliptical double-pipe heat exchanger through the simultaneous use of twisted tubes and non-Newtonian nanofluid. J Therm Anal Calorim. 2021;143:2825–40.
45. Shahsavar A, Rashidi M, Yıldız Ç, Arıcı M. Natural convection and entropy generation of Ag-water nanofluid in a finned horizontal annulus: A particular focus on the impact of fin numbers. Int Commun Heat Mass Transf. 2021;125:105349.
46. Yıldız Ç, Yıldız AE, Arıcı M, Azmi NA, Shahsavar A. Influence of dome shape on flow structure, natural convection and entropy generation in enclosures at different inclinations: a comparative study. Int J Mech Sci. 2021;197:106321.
47. Hussain S, Jamal M, Maatki C, Ghachem K, Kolsi L. MHD mixed convection of Al_2O_3–Cu–water hybrid nanofluid in a wavy channel with incorporated fixed cylinder. J Therm Anal Calorim. 2021;144:2219–33.
48. Ghachem K, Aich W, Kolsi L. Computational analysis of hybrid nanofluid enhanced heat transfer in cross flow micro heat exchanger with rectangular wavy channels. Case Studies in Thermal Engineering. 2021;24:100822.
49. Sundar LS, Sharma KV. Turbulent heat transfer and friction factor of Al_2O_3 nanofluid in circular tube with twisted tape inserts. Int J Heat Mass Transf. 2010;53:1409–16.
50. Huminic G, Huminic A. The heat transfer performances and entropy generation analysis of hybrid nanofluids in a flattened tube. Int J Heat Mass Transf. 2018;119:813–27.
51. Hazbehian M, Mohammadiun M, Maddah H, Alizadeh M. Analyses of exergy efficiency for forced convection heat transfer in a tube with CNT nanofluid under laminar flow conditions. Heat Mass Transf. 2017;53:1503–16.
52. Bejan A. Advanced Engineering Thermodynamics. New York: Wiley Interscience; 1988.
53. Sundar LS, Mesfin S, Ramana EV, Said Z, Sousa ACM. Experimental investigation of thermo-physical properties, heat transfer, pumping power, entropy generation, and exergy efficiency of nanodiamond+Fe_3O_4/60:40% water-ethylene glycol hybrid nanofluid flow in a tube. Therm Sci Eng Process. 2021;21:100799.
54. Sundar LS, Ramana EV, Graça MPF, Singh MK, Sousa ACM. Nanodiamond-Fe_3O_4 nanofluids: Preparation and measurement of viscosity, electrical and thermal conductivities. Int Commun Heat Mass Transf. 2016;73:62–74.
55. Akhavan-Behabadi MA, Shahidi M, Aligoodarz MR. An experimental study on heat transfer and pressure drop of MWCNT–water nano-fluid inside horizontal coiled wire inserted tube. Int Commun Heat Mass Transf. 2015;63:62–72.
56. Gnielinski V. New equations for heat and mass transfer in turbulent pipe and channel flow. Int Chem Eng. 1976;16:359–68.
57. Blasius H. The boundary layers in fluids with little friction. Z Math Phys. 1908;56:1–37.
58. Sundar LS, Bhramara P, Ravi Kumar NT, Singh MK, Sousa ACM. Experimental heat transfer, friction factor and effectiveness analysis of Fe_3O_4 nanofluid flow in a horizontal plain tube

with return bend and wire coil inserts. Int J Heat Mass Transf. 2017;109:440–53.
59. Keklikcioglu O, Ozceyhan V. Experimental investigation on heat transfer enhancement of a tube with coiled-wire inserts installed with a separation from the tube wall. Int Commun Heat Mass Transf. 2016;78:88–94.
60. Garcia A, Vicente PG, Viedma A. Experimental study of heat transfer enhancement with wire coil inserts in laminar-transition-turbulent regimes at different Prandtl numbers. Int J Heat Mass Transf. 2005;48:4640–51.
61. Kline SJ, McClintock FA. Describing uncertainties in single sample experiments. Mech Eng. 1953;75(1):3–8.